UNIVERSITÀ
DI PAVIA

Dipartimento di Fisica

Corso di laurea magistrale in Scienze fisiche

Theory and Simulation of Fractional Brownian Motion

Teoria e Simulazione del Moto Browniano Frazionario

Tesi per la laurea di:

Mircea Alexandru Codrea

Relatore:

Prof. Guido Montagna

Anno accademico 2025 – 2026

Abstract: Many complex systems in nature and society are not memoryless (i.e. Markovian) but they exhibit correlations or long-range dependence and are often characterized by anomalous diffusion. A non-Markovian stochastic process capable of capturing these features is fractional Brownian motion (fBM), introduced by Mandelbrot and van Ness (1968). Fields of application of fBM include biology, computer science, fluid dynamics, geophysics, and finance. Empirical studies of financial time series show evidence of memory, which motivates the use of fBM to model the autocorrelations of financial returns and volatility. The main aim of this thesis is to illustrate the theory of fBM-driven processes, validate their emergent statistical properties and investigate the implication of memory in financial returns for option pricing. The analyses were carried out by comparing theoretical results with data generated using one of the main fBM simulation algorithms (Davies-Harte). They highlight the Hurst parameter as a measure of correlation, confirm the Gaussian nature of fBM, the variance scaling property and the presence of long-range autocorrelation among the process increments. Moreover, introducing correlation into financial returns affects the valuation of financial derivatives, with a consequent decrease in option prices. Overall, the results provide a model that, compared with the classical memoryless framework, offers closer adherence to the phenomenology observed in financial markets.

Sommario: Molti sistemi complessi nella natura e nella società non sono senza memoria (Markoviani) ma esibiscono correlazioni o long-range dependence e sono spesso caratterizzati da una diffusione anomala. Un processo stocastico non Markoviano capace di catturare questi aspetti è il fractional Brownian motion (fBM), proposto da Mandelbrot e van Ness (1968). Campi di applicazione del fBM includono la biologia, la computer science, la fluidodinamica, la geofisica e la finanza. Attualmente, gli studi empirici sulle serie storiche finanziarie evidenziano la presenza di memoria, il che giustifica l'utilizzo del fBM per modellare le autocorrelazioni dei rendimenti e della volatilità. Il principale obiettivo di questa tesi è illustrare la teoria dei processi fBM-driven, verificare le proprietà statistiche emergenti e indagare le implicazioni sull'option pricing della presenza di memoria nei rendimenti finanziari. Le analisi sono state effettuate confrontando i risultati teorici con i dati generati mediante uno dei principali algoritmi di simulazione del fBM (Davies-Harte). Queste evidenziano il parametro di Hurst come misura della correlazione, confermano la natura Gaussiana del fBM, la proprietà di scaling della varianza e la presenza di autocorrelazione a lungo raggio tra gli incrementi del processo. Inoltre, l'introduzione della correlazione nei rendimenti finanziari influisce sulla valutazione dei derivati finanziari, con conseguente diminuzione dei prezzi delle opzioni. I risultati ottenuti forniscono un modello che rispetto a quello classico, privo di memoria, è capace di maggiore aderenza alla fenomenologia osservata nei mercati finanziari.

Contents

Introduction

Mathematical modeling of complex systems, in both physical and socio-economic domains, has historically relied on the memoryless assumption, formalised by the concept of a Markovian process. One of the primary stochastic processes used to model these phenomena is classical Brownian Motion (BM), described independently by Einstein and Langevin in the first decade of the twentieth century. However, the classical assumption of memorylessness stands in contrast to empirical phenomenology. In both natural and social contexts, systems exhibit behaviors, such as temporal correlations and anomalous diffusion, that Markovian processes can not replicate.

To overcome this limitation, Mandelbrot and van Ness introduced fractional Brownian motion (fBM) in 1968. This continuous-time Gaussian stochastic process generalises classical BM by introducing correlations between the increments of its realizations, making it particularly well-suited for describing non-Markovian systems. The degree of memory in the process is governed by a parameter $H \in [0, 1]$, known as the Hurst parameter. For $H = 0.5$, the process reduces to standard BM, reverting to a Markovian regime. On the other hand, for values above or below this threshold, the presence of memory alters the system dynamics, giving rise to persistent ($H > 0.5$) and anti-persistent ($H < 0.5$) regimes.

Due to its flexibility, fBM has found widespread applications across heterogeneous fields, such as biology, computer science, fluid dynamics, and geophysics. In recent decades, growing interest in the application of fBM has emerged within quantitative finance. Empirical analyses of market time series reveal the presence of statistical memory in the autocorrelations of financial returns and volatility. In particular, analyzing the Hurst parameter makes it possible to characterize the degree of market development, enabling a distinction between emerging markets, which exhibit persistent behavior, and mature ones, which display absence of memory or, to a lesser extent, anti-persistent behavior. Such empirical evidence makes classical models based on independent increments partially inadequate for capturing the actual behavior of the financial market dynamics, thus motivating

the study of fBM as an alternative to traditional models.

This thesis fits into this line of research and aims to present a comprehensive overview of the theory of fBM-driven processes, validate their emerging statistical properties via numerical simulations and investigate how the integration of long-range memory into financial returns impacts option pricing.

The first part of this work focuses on the numerical validation of the non-trivial statistical properties of fBM. Specifically, the thesis aims at verifying the Gaussian nature of the process, the scaling property of the variance, and the long-range autocorrelation structure of its increments through numerical simulations. The latter highlight the role of the Hurst parameter as a measure of correlation and anomalous diffusion. To this end, sample paths of the fBM are simulated to generate the dataset required for the empirical analysis. This is achieved using the Davies-Harte algorithm, which was selected for its computational efficiency and is widely recognized as one of the primary methods in the literature.

Subsequently, the thesis examines the implications of adopting non-Markovian processes as a foundation for modeling financial returns. To this end, geometric fractional Brownian motion (GfBM) is introduced and numerically validated before being employed to implement a generalized Black-Scholes model for option pricing and delta hedging. The key aim is to evaluate how persistent regime influences the fair value of call options.

To present the study systematically, this thesis is structured into four chapters, organized as follows:

Chapter 1 - Markov Stochastic Processes introduces the theoretical framework of memoryless stochastic processes, reviewing the formulations of Brownian motion developed by Einstein and Langevin. It presents the general classification of processes, the Fokker-Planck equation, and the rigorous formalization of the Wiener process, concluding with the foundations of Itô stochastic calculus and the formulation of stochastic differential equations (SDEs).

Chapter 2 - Fractional Brownian Motion introduces the formal definition of fBM and its self-similarity properties governed by the Hurst parameter H. It analyzes Fractional Gaussian Noise (fGN) and its long-range autocorrelation, establishing the mathematical foundations of fractional stochastic calculus and the solution of the generalized Fokker-Planck equation.

Chapter 3 - Simulation of Fractional Brownian Motion analyzes the computational aspects of the process, describing the primary simulation algorithms (Cholesky decomposition, Hosking's algorithm, and the Davies-Harte method) and justifying the choice of the latter. It then details the methodology employed

to numerically validate the evolution of variance, convergence to the Gaussian distribution and the decay of increment correlation.

Chapter 4 - Geometric Fractional Brownian Motion presents the financial application of the model. After discussing the economic justification for adopting fBM, the analytical solution for GfBM is derived. This is followed by the validation via simulated sample paths and the development of the fractional Black-Scholes model, evaluating the impact of the Hurst parameter on call option pricing and Delta sensitivity.

Chapter 1

Markov Stochastic Processes

In this chapter, we introduce the theoretical framework of Markov stochastic processes, starting with the interpretations of Brownian Motion proposed by Einstein and Langevin and their underlying assumption of memorylessness. We then present the general classification of stochastic processes, highlighting the Fokker-Planck equation to model drift and diffusion dynamics. Next, we analyze the rigorous formalization of the Wiener process, emphasizing its autocorrelation function, scale invariance, and its continuity and non-differentiability of trajectories. The discussion concludes with the formulation of stochastic differential equations (SDEs) and the fundamentals of stochastic calculus.

1.1 Brownian Motion: Einstein and Langevin Interpretation

Brownian motion takes its name from the botanist Robert Brown, who observed under a microscope the chaotic motion of pollen grains suspended in a liquid. This phenomenon, which occurs for virtually any type of particle immersed in a thermal bath at constant temperature, constitutes the macroscopic manifestation of the fluid's microscopic fluctuations.

Although experimental observations of this phenomenon were made in the first half of the nineteenth century, its rigorous theoretical formalization was achieved only at the beginning of the twentieth century. Albert Einstein and Paul Langevin proposed two distinct, yet statistically equivalent theoretical interpretations of Brownian motion. Einstein's interpretation uses a macroscopic and statistical approach, whereas Langevin's interpretation uses a microscopic and dynamic approach. Both, however, rely on a fundamental assumption: the

Markov property of the process, namely the absence of memory.

It is worth emphasizing that the modeling of Brownian motion had already been introduced completely independently a few years earlier by the French mathematician Louis Bachelier [1]. His work was aimed at studying fluctuations in the Paris stock exchange through a symmetric random-walk model. Bachelier's key insight was that the price of a stock fluctuates as the result of an enormous number of independent transactions, in close analogy with the way a particle moves under the effect of random impacts from the molecules of the surrounding fluid. With this pioneering contribution, Bachelier laid the foundations of modern econophysics and showed that models of statistical diffusion can have interdisciplinary applications, spanning both physical systems and financial markets.

Einstein's Probabilistic Interpretation

In one of his celebrated papers from his *annus mirabilis* (1905) [2], Albert Einstein interpreted Brownian motion within the framework of the kinetic theory of matter. Einstein's central idea is that a Brownian particle is continuously bombarded by the molecules of the surrounding fluid, which are in motion due to thermal agitation. These collisions drive the particle along a highly irregular trajectory.

He chose not to track the individual trajectories of the suspended particles; instead, he considered a statistical ensemble and analyzed the collective behavior of a large number of mutually independent Brownian particles immersed in a thermal bath at constant temperature.

Einstein's goal was to derive the time evolution of the probability density $p(x,t)$ of finding a particle at position x at time t. Such evolution is governed by the diffusion equation that bears his name:

$$\partial_t p(x,t) = D\partial_x^2 p(x,t) \tag{1.1}$$

with D denoting the macroscopic diffusion coefficient. The explicit expression for this coefficient, known as the Einstein-Smoluchowski relation, was derived in a subsequent work by Einstein. It relates the macroscopic diffusion coefficient to the microscopic properties of the system.

To obtain the dynamical law for the probability density (1.1), Einstein assumed that the microscopic motion was governed by a series of random displacements so called "jumps" occurring over a characteristic time scale τ. The assumptions underlying the model are that:

a. The observation time scale t is much larger than the characteristic jump time τ;

b. The characteristic time τ is sufficiently large so that successive jumps performed by a particle are statistically independent.

The latter assumption implicitly encodes the Markovian nature of the model. Assuming that the process is memoryless means assuming that to know the future spatial distribution of the system at time $t + \tau$, it is sufficient to know only the present distribution at time t. In other words, the trajectory followed by the particle to reach its current position does not affect the next jump.

Langevin's Dynamic Interpretation

A few years after Einstein's work was published, in 1908 [3], the physicist Paul Langevin proposed an alternative model for the description of Brownian motion, one that focused on a microscopic and dynamical description. Langevin's central idea was to describe the system's evolution by studying the trajectory $x(t)$ of a single Brownian particle suspended in the liquid. To this end, he applied the laws of classical mechanics, expressed in the form of Newton's second law of motion.

Langevin modeled the microscopic dynamics assuming that the total forces acting on the particle were the combination of two distinct contributions: a deterministic viscous force, $F_1 = -6\pi\eta r v$, which opposes the particle motion, and a fluctuating stochastic force, $F_2 = \xi(t)$. The latter, commonly referred to as White (or Gaussian) Noise, models the countless microscopic impacts arising from the thermal agitation of molecules.

Langevin's goal was to use Newton's second law of motion to write a differential equation for the particle's velocity; he thus wrote one of the first stochastic differential equations:

$$m\frac{dv(t)}{dt} = -6\pi\eta r v(t) + \xi(t) \tag{1.2}$$

From this equation, by means of appropriate averages over noise realizations, one derives the mean square displacement of the particles, i.e. the variance of the Brownian motion process. This approach proves to be statistically equivalent to Einstein's probabilistic description and leads to the same results.

To solve the equation, Langevin had to introduce fundamental assumptions regarding the statistical nature of the stochastic force:

a. The force has a zero mean value, $\langle \xi(t) \rangle = 0$, so that there are no privileged directions for molecular collisions;

b. The force is temporally independent, meaning that the autocorrelation at different times is proportional to a Dirac delta function:

$$\langle \xi(t)\xi(t') \rangle = \delta(t - t')$$

In this last assumption lies the Markovian nature of Langevin's model. Stating that White Noise is instantaneously uncorrelated means assuming that the process is memoryless. In fact, the impulse received by the Brownian particle at instant t is statistically independent of all collisions previously suffered. At every instant, the particle forgets the followed path, making future evolution dependent solely on the current state of the system.

The statistical equivalence between Langevin's dynamic formulation and Einstein's probabilistic formulation highlights how the assumption of Markov property is therefore the crucial conceptual point for the correct description of Brownian motion.

1.2 Classification and Markov Processes

To understand the properties of Markov processes, it is useful to formalize and review the theory of stochastic processes and their key characteristics [4].

Classification of Stochastic Processes

Denoting time by t and the value assumed by the random variable X by x, we can state the following definition of a stochastic process:

Definition 1.1. *A stochastic process is a family of random variables* $\{X(t), t \in T\}$ *indexed by a parameter* t.

Depending on the discrete or continuous nature of the time parameter $t \in T$, we can distinguish between:

- **Discrete-time stochastic processes** ($T = \mathbb{N}$): used, for instance, to describe the position of a random walker after n steps, $X(t = t_n) = x_n$, opening/closing stock prices, or daily average temperatures.
- **Continuous-time stochastic processes** ($T = \mathbb{R}_+$): used, for example, to describe the position $X(t) = x(t)$ of a Brownian particle (Einstein's formulation) or its velocity $X(t) = v(t)$ (Langevin's formulation).

Definition 1.2. *A specific sequence of values assumed by x is called a realization or sample path (or trajectory) of the stochastic process $X(t)$. When such a realization originates from empirical observations, it is called a time series. The collection of all possible realizations is referred to as the ensemble (or phase space).*

We can therefore conclude that a stochastic process is characterized by an infinite family of functions that evolve randomly in time.

Definition 1.3. *The* joint probability density function $p(x_2, t_2; x_1, t_1) \doteq p_2$ *is defined as the probability density of observing the value x_1 at time t_1 and x_2 at time t_2. The n-point joint probability density is denoted by*

$$p(x_n, t_n; x_{n-1}, t_{n-1}; \dots; x_1, t_1) \doteq p_n$$

Starting from this definition, a stochastic process can be uniquely characterized using the following theorem due to Kolmogorov:

Theorem 1.1 (Kolmogorov Theorem)**.** *A stochastic process is uniquely determined if its finite-dimensional joint probability density is specified for every finite set of times $\{t_1, t_2, \dots, t_n\} \subseteq T$, satisfying the following properties:*

- ***Positivity:*** $p_n \geq 0$
- ***Symmetry:*** $p_n(\dots; x_i, t_i; \dots; x_j, t_j; \dots) = p_n(\dots; x_j, t_j; \dots; x_i, t_i; \dots)$
- ***Completeness:*** $\int p_n(x_n, t_n; \dots; x_1, t_1)\, dx_n = p_{n-1}(x_{n-1}, t_{n-1}; \dots; x_1, t_1)$
- ***Normalization:*** $\int p_1(x, t)\, dx = 1$

In the context of stochastic processes, further classifications can be achieved by imposing additional constraints.

Stationary Processes

A stochastic process is said to be *stationary* (or *strictly stationary*) if and only if, for every n and for any time shift Δt,

$$p_n(x_n, t_n + \Delta t; \dots; x_1, t_1 + \Delta t) = p_n(x_n, t_n; \dots; x_1, t_1)$$

that is, if its joint probability densities are invariant under time translations. Consequently, suitable transformations can be applied to make them independent of absolute time,

$$p_n(x_n, t_n; \dots; x_1, t_1) \Rightarrow p(x_n; \dots; x_1)$$

Random Processes

A stochastic process is said to be *purely random* if and only if, for all n and for any sequence of times $t_1 \leq t_2 \leq \cdots \leq t_n$,

$$p(x_n, t_n \mid x_{n-1}, t_{n-1}; \ldots; x_1, t_1) = p(x_n, t_n) \implies p(x_n, t_n; \ldots; x_1, t_1) = \prod_{i=1}^{n} p(x_i, t_i)$$

where

$$p(x_n, t_n \mid x_{n-1}, t_{n-1}; \ldots; x_1, t_1) \doteq \frac{p_n(x_n, t_n; \ldots; x_1, t_1)}{p_{n-1}(x_{n-1}, t_{n-1}; \ldots; x_1, t_1)} \tag{1.3}$$

is the *conditional probability density function*, which for $n = 2$ reduces to the standard definition of conditional probability (or Bayes rule). In such a process, future states are not conditioned by past events or by the present state but they are completely independent.

Markov Processes

A stochastic process is said to be a *Markov process* (or to satisfy the *Markov property*) if and only if, for all n and for any sequence of times $t_1 \leq t_2 \leq \cdots \leq t_n$,

$$p(x_n, t_n \mid x_{n-1}, t_{n-1}; \ldots; x_1, t_1) = p(x_n, t_n \mid x_{n-1}, t_{n-1})$$

that is, knowledge of the present state completely determines the future evolution of the system, making the process independent of its past (memoryless).

Chapman-Kolmogorov Equation

Consider a chronological sequence of times $t_1 \leq t_2 \leq \cdots \leq t_n$. From equation (1.3), the conditional probability density function is evaluated given $n-1$ fixed values. Inverting this relation, we can express the joint probability density function in terms of the conditional one:

$$p(x_n, t_n; \ldots; x_1, t_1) = p(x_n, t_n \mid x_{n-1}, t_{n-1}; \ldots; x_1, t_1) p(x_{n-1}, t_{n-1}; \ldots; x_1, t_1) \tag{1.4}$$

If the underlying stochastic process is memoryless, we can apply the Markov property to rewrite the joint probability density function in terms of the transition probability density:

$$p(x_n, t_n; \ldots; x_1, t_1) = p(x_n, t_n \mid x_{n-1}, t_{n-1}) p(x_{n-1}, t_{n-1}; \ldots; x_1, t_1) \tag{1.5}$$

By repeating this reduction step recursively, we observe that:

$$\begin{aligned} p(x_{n-1}, t_{n-1}; \ldots; x_1, t_1) &= p(x_{n-1}, t_{n-1} \mid x_{n-2}, t_{n-2}) p(x_{n-2}, t_{n-2}; \ldots; x_1, t_1) \\ &\vdots \\ p(x_2, t_2; x_1, t_1) &= p(x_2, t_2 \mid x_1, t_1) p(x_1, t_1) \end{aligned}$$

Substituting these expressions back into (1.5) yields:

$$p(x_n, t_n; \ldots; x_1, t_1) = p(x_1, t_1) \prod_{j=2}^{n} p(x_j, t_j \mid x_{j-1}, t_{j-1}) \tag{1.6}$$

Thus, for a Markov process, the joint probability density is fully determined by the initial marginal probability density and the product of the two-point transition probability densities. Considering the specific case for $n = 3$, equation (1.6) reduces to:

$$p(x_3, t_3; x_2, t_2; x_1, t_1) = p(x_3, t_3 \mid x_2, t_2) p(x_2, t_2 \mid x_1, t_1) p(x_1, t_1) \tag{1.7}$$

Since x_2 represents an intermediate state along the trajectory, and the evolution of interest is the overall transition from x_1 to x_3, we can integrate over all possible values of x_2:

$$\int p(x_3, t_3; x_2, t_2; x_1, t_1)\, dx_2 = p(x_1, t_1) \int p(x_3, t_3 \mid x_2, t_2) p(x_2, t_2 \mid x_1, t_1)\, dx_2 \tag{1.8}$$

Note that the left-hand side of (1.8) corresponds to the marginal joint probability density $p(x_3, t_3; x_1, t_1)$, which can be expressed via the Bayes rule as:

$$p(x_3, t_3; x_1, t_1) = p(x_3, t_3 \mid x_1, t_1) p(x_1, t_1) \tag{1.9}$$

Equating (1.8) and (1.9) and canceling out the non-zero marginal probability $p(x_1, t_1)$, we obtain the Chapman-Kolmogorov (CK) equation:

$$p(x_3, t_3 \mid x_1, t_1) = \int p(x_3, t_3 \mid x_2, t_2) p(x_2, t_2 \mid x_1, t_1)\, dx_2 \tag{1.10}$$

Remark 1.1. *The CK equation, which holds exclusively for Markov processes, is closely related to the equation proposed by Einstein in his seminal paper on*

Brownian motion [2] and used to model jump probabilities:

$$p(x, t+\tau) = \int d\Delta\, \phi(\Delta)\, p(x+\Delta, t)$$

This indicates that he had implicitly assumed the underlying stochastic process to be Markovian.

1.3 Fokker-Planck Equation

The Fokker-Planck (FP) equation is a partial differential equation of fundamental importance in statistical physics, econophysics and finance [5]. It describes the time evolution of the probability density $p(x, t \mid x_0, t_0)$ of a system governed by a continuous time Markovian process.

Derivation of the Fokker-Planck Equation

The mathematical derivation of FP equation relies on that of Chapman and Kolmogorov. Assuming the following time ordering, $t_0 < t < t+\tau$, where $\tau \ll t - t_0$ is an infinitesimal time interval, the CK integral equation (1.10) becomes:

$$p(x, t+\tau \mid x_0, t_0) = \int \mathrm{d}x'\, p(x, t+\tau \mid x', t)\, p(x', t \mid x_0, t_0) \tag{1.11}$$

The objective is to derive a differential equation for the time evolution of the transition probability density. To achieve this, one must first obtain an expansion of the time derivative of the transition probability density, known as the Kramers-Moyal expansion.

Kramers-Moyal Expansion

1. Subtracting from both sides of equation (1.11) the term $p(x, t \mid x_0, t_0)$ that is, the limit of the transition probability density as $\tau \to 0$ we obtain:

$$p(x, t+\tau \mid x_0, t_0) - p(x, t \mid x_0, t_0) =$$
$$\int \mathrm{d}x'\, p(x, t+\tau \mid x', t) p(x', t \mid x_0, t_0) - p(x, t \mid x_0, t_0)$$

2. Dividing both sides of the equation by the infinitesimal time interval τ and

taking the limit $\tau \to 0$, the left-hand side becomes a partial derivative:

$$\partial_t p(x,t \mid x_0,t_0) = \lim_{\tau\to 0} \frac{1}{\tau}\left[\int \mathrm{d}x'\, p(x,t+\tau \mid x',t)p(x',t \mid x_0,t_0) - p(x,t \mid x_0,t_0)\right]$$

3. We can use the Taylor expansion on the integrand, which depends on x'. Furthermore, we can perform a change of integration variable by introducing a jump variable $\Delta \doteq x - x'$. In this way, the integrand is expressed in terms of the starting point x. The equation then becomes:

$$p(x,t+\tau \mid x',t)p(x',t \mid x_0,t_0) = \sum_{m=0}^{\infty} \frac{(-1)^m}{m!}\Delta^m \partial_x^m \left[p(x'+\Delta,t+\tau \mid x',t)p(x',t \mid x_0,t_0)\right]$$

4. Substituting this expression into the integral, performing the integration, and factoring out the terms independent of the jump variable Δ, we define the Kramers-Moyal coefficients:

$$a_m(x,t) \doteq \lim_{\tau\to 0} \frac{1}{\tau} \int \mathrm{d}\Delta\, \Delta^m p(x+\Delta,t+\tau \mid x,t) \tag{1.12}$$

5. This makes it possible to write the Kramers-Moyal expansion as an infinite order linear differential equation:

$$\partial_t p(x,t \mid x_0,t_0) = \sum_{m=1}^{\infty} \frac{(-1)^m}{m!} \partial_x^m \left(a_m(x,t)p(x,t \mid x_0,t_0)\right) \tag{1.13}$$

This type of differential equation is generally impossible to solve analytically, hence requiring a truncation of the series to reduce its order. A crucial role in this procedure is played by Pawula's theorem, which establishes a fundamental rule: if the Kramers-Moyal series is truncated at a finite order greater than two, the resulting probability density can take negative values, violating the postulates of probability and leading to unphysical solutions. Truncating the expansion at second order, instead, yields the Fokker-Planck equation [5]:

$$\partial_t p(x,t \mid x_0,t_0) = -\partial_x \left[a_1(x,t)p(x,t \mid x_0,t_0)\right] + \frac{1}{2}\partial_x^2 \left[a_2(x,t)p(x,t \mid x_0,t_0)\right] \tag{1.14}$$

The same reasoning can be applied to the marginal probability density $p(x,t)$ by integrating over the initial position, leading to a similar result.

Interpretation of the Fokker-Planck Equation

Considering now the FP equation for the marginal probability density:

$$\partial_t p(x,t) = -\partial_x \left[a_1(x,t)p(x,t)\right] + \frac{1}{2}\partial_x^2 \left[a_2(x,t)p(x,t)\right] \tag{1.15}$$

the physical meaning of the two remaining Kramers-Moyal coefficients can easy be deduced. This can be achieved by determining the time evolution of the mean value and the variance of the underlying stochastic process. This derivation relies on the FP equation under the assumption that the probability density $p(x,t)$, together with its spatial derivatives, vanishes sufficiently fast at infinity.

- **Drift Coefficient**
  If we take in consideration the time evolution of the mean value. Assuming for simplicity a constant coefficient $a_1(x,t) = a_1$:

  $$\frac{\mathrm{d}}{\mathrm{d}t}\langle x(t)\rangle = \frac{\mathrm{d}}{\mathrm{d}t}\int_{-\infty}^{+\infty} x\, p(x,t)\,\mathrm{d}x = \int_{-\infty}^{+\infty} x\, \partial_t p(x,t)\,\mathrm{d}x$$

  By substituting the FP equation and integrating by parts, one can show that:

  $$\frac{\mathrm{d}}{\mathrm{d}t}\langle x(t)\rangle = a_1 \implies \langle x(t)\rangle = \langle x(0)\rangle + a_1 t$$

  We observe that a_1 represents the average translation velocity of the system and is referred to as the drift coefficient. A constant drift shifts the mean of the distribution over time without altering its shape.

- **Diffusion Coefficient**
  Let us now consider the time evolution of the variance. In the absence of drift ($a_1(x,t) = 0$), and assuming a constant coefficient $a_2(x,t) = a_2$, substituting the FP equation yields:

  $$\frac{\mathrm{d}}{\mathrm{d}t}\langle x^2(t)\rangle = a_2 \implies \langle x^2(t)\rangle = \langle x^2(0)\rangle + a_2 t$$

  Consequently, the variance evolves according to:

  $$\mathrm{Var}[x(t)] = \langle x^2(t)\rangle - \langle x(t)\rangle^2 = \mathrm{Var}[x(0)] + a_2 t$$

  In this specific case, we observe that the coefficient a_2 quantifies the strength of the stochastic fluctuations acting on the system, governing the rate of dispersion and broadening of the probability distribution. For this reason, it

is referred to as the diffusion coefficient. Note that, under constant diffusion, the variance increases linearly with time.

Depending on the functional form assumed by the coefficients $a_1(x,t)$ and $a_2(x,t)$, the FP equation describes several fundamental processes:

Einstein-Wiener Process

Assuming zero drift ($a_1(x,t) = 0$) and a constant diffusion coefficient ($a_2(x,t) = 1$ or $2D$), we obtain a stochastic process that describes classical Brownian motion or pure diffusion.

Fick Process

For constant drift ($a_1(x,t) = v$) and constant diffusion ($a_2(x,t) = D$), the process models an asymmetric (biased) random walk or mass transport with diffusion.

Ornstein-Uhlenbeck Process

By choosing a drift coefficient linear in position ($a_1(x,t) = -\gamma x$, with $\gamma > 0$) together with a constant diffusion coefficient ($a_2(x,t) = D$), we obtain a mean-reverting process. This is used to describe the velocity of Brownian particles, interest rate dynamics and stochastic volatility.

Geometric Brownian Motion

Assuming more complex functional forms to both coefficients such as a linear drift ($a_1(x,t) = \mu x$, with $\mu > 0$) and a quadratic diffusion coefficient ($a_2(x,t) = \sigma^2 x^2$) the process represents the standard Samuelson model, which serves as the foundation for model stock price dynamics in quantitative finance.

1.4 Wiener Process or Brownian Motion

The Wiener process, also known as Brownian motion, represents the rigorous formalization of the Brownian motion studied by Einstein, and is usually denoted by $W(t)$ (or $B(t)$). Originally introduced to study the motion of a microscopic particle suspended in a fluid, today it is also widely used in econophysics to model financial markets.

Connection with Fokker-Planck Equation and Formal Definition

The Wiener process is closely linked to the statistical description of dynamical systems. In his work [6], Wiener attempts to interpret and analyze Einstein's diffusion equation from the perspective of the Fokker-Planck equation.

Considering 1.14 and assuming a system with no external forces ($a_1(x,t) = 0$) and a constant fluctuation intensity ($a_2(x,t) = 1$), we obtain Einstein's pure diffusion equation (with a diffusion coefficient of $D = \frac{1}{2}$):

$$\partial_t p(x,t|x_0,t_0) = \frac{1}{2}\partial_x^2 p(x,t|x_0,t_0)$$

For the initial condition $p(x,t_0|x_0,t_0) = \delta(x-x_0)$ (representing absolute certainty regarding the position of the system at the initial time) the fundamental solution is the conditional probability density:

$$p(x,t|x_0,t_0) = \frac{1}{\sqrt{2\pi(t-t_0)}} e^{-\frac{(x-x_0)^2}{2(t-t_0)}} \tag{1.16}$$

This solution characterizes the Wiener process and represents the probability density of finding the system at position x at time t, given absolute certainty that it was at position x_0 at time t_0.

This solution can be interpreted as a marginal probability density. By considering the probability of the system transitioning from (x_{i-1}, t_{i-1}) to (x_i, t_i), one can define a position increment $x_i - x_{i-1} \doteq \Delta x_i$ occurring over a time interval $t_i - t_{i-1} \doteq \Delta t_i$. Performing a change of variables yields the marginal probability density of the Wiener increments:

$$p(\Delta x_i, \Delta t_i) = \frac{1}{\sqrt{2\pi\Delta t_i}} e^{-\frac{\Delta x_i^2}{2\Delta t_i}}$$

Below, we provide a formal definition of the process:

Definition 1.4. *A continuous time stochastic process $\{W(t), t \geq 0\}$ is defined as a Wiener process if it satisfies the following properties:*

1. ***Initial condition.*** *The process starts almost surely at zero:*

$$W(0) = 0 \quad \textit{(a.s.)}$$

2. ***Continuity of sample paths.*** *The sample paths $t \mapsto W(t)$ are almost*

surely continuous functions of time (i.e., they display no discrete jumps).

3. ***Independent increments.*** *For any sequence of time instants* $0 \leq t_0 < t_1 < \cdots < t_n$*, the successive increments*

$$\Delta W_i = W(t_i) - W(t_{i-1})$$

are mutually independent random variables. Thus, knowledge of past evolution provides no information about future increments (Markov property).

4. ***Gaussian and stationary increments.*** *For every pair of times* $0 \leq s < t$*, the increment* $W(t) - W(s)$ *follows a Gaussian distribution with zero mean and variance equal to the time interval:*

$$W(t) - W(s) \sim \mathcal{N}(0, t - s)$$

Stationarity implies that the distribution depends solely on the duration of the time interval $t - s$ *and not on the initial time* s*.*

From this formalization, it is possible to derive the autocorrelation function of a Wiener process $W(t)$. The resulting relation yields the autocorrelation between any two arbitrary time instants and is entirely determined by the smaller of the two:

$$\langle W(t)W(s)\rangle = \min(t, s) \tag{1.17}$$

Although future increments of Brownian motion are completely independent (a fundamental aspect of its Markovian nature), the positions occupied by the Wiener process at different time instants remain positively correlated. This relation indicates that the trajectory retains a "memory", as future states are influenced by preceding positions.

Scale Invariance and Non-Differentiability of Sample Paths

Realizations of the Wiener process possess the geometric properties of a one-dimensional Gaussian fractal. One of these properties is scale invariance, or self-similarity. If we apply the Gaussian scaling relations

$$\begin{cases} (t - t_0) \to (\hat{t} - \hat{t}_0) = b(t - t_0) \\ (x - x_0) \to (\hat{x} - \hat{x}_0) = b^{1/2}(x - x_0) \end{cases}$$

to transform the conditional probability density 1.15, we obtain:

$$p(x,t|x_0,t_0) \to p_G(\hat{x},\hat{t}|\hat{x}_0,\hat{t}_0) = b^{-1/2}p(x,t|x_0,t_0)$$

Furthermore, it can be verified that the resulting probability density (p_G) preserves both the normalization and the statistical properties of the process. This invariance under Gaussian scaling implies that the trajectories retain the same qualitative and statistical characteristics regardless of the temporal or spatial interval considered. As highlighted by Mandelbrot, the absence of a characteristic scale makes the Wiener process a continuous fractal whose structure is preserved. Zooming in on any portion of the fractal reveals the same detailed structure visible on a global scale.

If a curve is a fractal, its structure remains rough and fluctuating at every scale. The persistence of these fluctuations at infinitely small scales precludes the possibility of defining a time derivative, leading to the almost sure non-differentiability of the paths.

Analysis of the average velocity of a trajectory over a given time interval reveals divergent behavior. It can be shown that the probability of the average velocity exceeding a given threshold K depends on the complementary error function and is expressed as:

$$\text{Prob}\left\{\left|\frac{\Delta W}{\Delta t}\right| > K\right\} = \text{erfc}\left(K\sqrt{\frac{\Delta t}{2}}\right)$$

Taking the limit as $\Delta t \to 0$, we observe that:

$$\lim_{\Delta t\to 0} \text{erfc}\left(K\sqrt{\frac{\Delta t}{2}}\right) = \text{erfc}(0) = 1$$

This limit holds for an arbitrarily large value of K, even as $K \to \infty$. Therefore, the derivative cannot be defined at any point. Consequently, the sample paths of the Wiener process are almost surely everywhere continuous and nowhere differentiable.

Physically, this implies that the instantaneous velocity of the Brownian particle diverges to infinity. Since an infinite velocity is unphysical, it becomes necessary to resort to alternative formulations for describe velocity and to establish a dedicated mathematical framework, known as stochastic calculus, to handle the differentials of such processes.

1.5 Stochastic Calculus and SDEs

Stochastic calculus was developed to address the limitations of classical theory in describing phenomena characterized by continuous and irregular microscopic fluctuations, such as those governing the Wiener process used to describe the motion of Brownian particles [4].

In particular, as discussed in the previous section, the Wiener process generates trajectories with fractal properties that are almost surely continuous everywhere but nowhere differentiable. This prevents the description of the velocity of the system through the standard definition of the derivative, which diverges, hence highlighting the inadequacy of ordinary differentiability.

Stochastic Differential Equations

In an attempt to model dynamical systems subject to stochastic fluctuations, as discussed in section 1.1, was historically introduced the Langevin equation:

$$\frac{dx}{dt} = a(x,t) + b(x,t)\xi(t)$$

where $\xi(t)$ denotes white noise. Mathematically, it is defined as a continuous time Gaussian stochastic process with zero mean and a time autocorrelation witch is a function expressed by a Dirac delta function:

$$\langle \xi(t)\xi(t') \rangle = \delta(t - t')$$

Consequently, white noise is a mathematical abstraction describing a process with unbounded fluctuations, making it impossible to treat using standard differential calculus. For this reason, it is natural to seek a connection between white noise $\xi(t)$ and the Wiener process $W(t)$.

It can be shown that applying the time-derivative operator to the autocorrelation of the Wiener process 1.17 yields the white noise autocorrelation:

$$\langle dW(t)dW(t') \rangle = \langle \xi(t)\xi(t') \rangle \, dt \, dt' \tag{1.18}$$

From this statistical identity, follows the formal expression (understood in the distributional sense):

$$dW(t) = \xi(t)\, dt$$

Furthermore, since equation 1.18 is equivalent to $\langle dW(t)dW(t') \rangle = \delta(t - t')\, dt\, dt'$, it ensures that the autocorrelation of the Wiener increments is preserved

even for infinitesimal increments:

- for $t = t' \implies \langle dW^2(t) \rangle = dt$;
- for $t \neq t' \implies \langle dW(t) dW(t') \rangle = 0$.

This formalism allows the Langevin equation to be interpreted as a primary example of a Stochastic Differential Equation (SDE) [4]:

$$dx(t) = a(x,t)\, dt + b(x,t)\, dW(t) \tag{1.19}$$

It is essential to emphasize that this is merely a shorthand notation, as $dW(t)$ lacks a rigorous differential meaning and can be defined rigorously only through integral notation:

$$x(t) = x(t_0) + \int_{t_0}^{t} a(x,t')\, dt' + \int_{t_0}^{t} b(x,t')\, dW(t')$$

While the first integral is a standard classical, the second is a stochastic integral with respect to the increments of the Wiener process, the evaluation of which requires the formulation of a new calculus [7].

Stochastic Calculus

A stochastic integral is formally expressed as:

$$S = \int_{t_0}^{t} G(t')\, dW(t')$$

In this expression, the integrand $G(t')$ represents a function, which may itself be a stochastic process. Due to the irregular nature of the Wiener process increments $dW(t')$, the integral cannot be evaluated using traditional calculus, requiring instead a probabilistic construction.

To rigorously define the stochastic integral over the time interval $[t_0, t]$, we introduce a partition of the interval into M subintervals $t_0 < t_1 < t_2 < \cdots < t_M = t$. Within each subinterval, a generic evaluation point τ_i is chosen such that $t_{i-1} \leq \tau_i \leq t_i$. Based on this partition, the discrete stochastic sum S_M is defined as:

$$S_M = \sum_{i=1}^{M} G(\tau_i)\, \Delta W_i$$

It should be noted that the Wiener increments make this sum itself a random variable. Furthermore, while in classical integration the choice of τ_i does not

affect the limiting value of the sum, in stochastic integration the selection of this evaluation point is crucial.

If the evaluation point is expressed by introducing a parameter $\alpha \in [0, 1]$ such that $\tau_i = \alpha t_i + (1 - \alpha)t_{i-1}$, it can be shown that the expectation value of the stochastic sum depends directly on α:

$$\langle S_M \rangle = \alpha(t - t_0)$$

The dependence of the mean on α reveals that varying this parameter yields infinitely many possible definitions for the stochastic integral. This leads to two primary conventions:

a. **Itô integral ($\alpha = 0$):** The evaluation point is fixed at the left endpoint of each subinterval, $\tau_i = t_{i-1}$. In this configuration, the integrand is evaluated before the Wiener increment occurs, preserving the non-anticipative nature of the process.

b. **Stratonovich integral ($\alpha = 1/2$):** The evaluation point is set to the midpoint of the interval, $\tau_i = \frac{t_{i-1}+t_i}{2}$. This symmetric choice preserves the standard rules of integration and differentiation from classical Riemannian calculus.

Once the discretization convention is established by fixing the parameter α, it is necessary to define the limit operator of the stochastic sum S_M as the number of subintervals approaches infinity ($M \to \infty$). Since we are dealing with probabilistic quantities, the convergence of the sum S_M to the stochastic integral S is imposed via the mean-square limit criterion:

$$S = \underset{M\to\infty}{\text{ms-lim}}\, S_M \iff \lim_{M\to\infty} \left\langle (S_M - S)^2 \right\rangle = 0$$

By choosing the convention $\alpha = 0$, the Itô stochastic integral exhibits several algebraic properties. Assuming that the processes $G(t)$ and $H(t)$ are non-anticipative functions, meaning that for any time $t' \leq s$, their value evaluated at t' is statistically independent of the Wiener process increment $W(s) - W(t')$, it can be shown that the following:

1. **Mean Value Property:**

$$\left\langle \int_{t_0}^{t} G(t')\, dW(t') \right\rangle = 0$$

2. **Correlation Formula:**

$$\left\langle \int_{t_0}^{t} G(t')\, dW(t') \int_{t_0}^{t} H(s)\, dW(s) \right\rangle = \int_{t_0}^{t} \langle G(t')H(t') \rangle\, dt'$$

3. **Quadratic Variation of the Wiener Process:** Understood in the mean-square limit sense, the following equality holds:

$$(dW(t))^2 = dt$$

More generally, for higher powers or mixed products, this leads to:

$$[dW(t)]^{2+N} = 0 \quad \forall N > 0$$
$$dW(t)\, dt = 0$$

4. **Itô's Lemma:** Consider a continuous stochastic process $x(t)$ governed by 1.19, and let $f(x,t)$ be a scalar function differentiable at least up to second order with respect to the spatial variable x, and to first order with respect to time t. The stochastic differential evolution of the composite function, expressed as $df[x(t),t]$, is given by [7]:

$$df[x(t),t] = \left\{ \frac{\partial f}{\partial t} + a(x,t)\frac{\partial f}{\partial x} + \frac{1}{2}b^2(x,t)\frac{\partial^2 f}{\partial x^2} \right\} dt + b(x,t)\frac{\partial f}{\partial x}\, dW(t)$$

Remark 1.2. *Compared to the classical rules of ordinary calculus, an additional corrective term appears:* $\frac{1}{2}b^2(x,t)\frac{\partial^2 f}{\partial x^2}$. *This term captures the effect of microscopic fluctuations along the stochastic path, which contribute macroscopically to the deterministic drift.*

This mathematical framework forms the cornerstone of stochastic calculus applications across various fields, including statistical physics and quantitative finance.

Chapter 2

Fractional Brownian Motion

In this chapter, we introduce Fractional Brownian Motion (fBM) [8], describing its fundamental properties and self-similarity governed by the Hurst parameter H[1]. We then analyze Fractional Gaussian Noise (fGN), highlighting the stationarity of its increments and the long-range autocorrelation associated with the non-Markovian memory of the process. The discussion concludes with the formulation of fractional stochastic differential equations (fSDE) and the solution of the generalized Fokker-Planck equation.

2.1 Definition and properties of fBM

Definition 2.1. *Fractional Brownian motion (fBM) with Hurst parameter (or index) $H \in (0,1) \subset \mathbb{R}$ is a continuous-time Gaussian stochastic process $\{B_H(t), t \geq 0\}$. It is characterized by:*

- *initial value: $B_H(0) = 0$ almost surely;*
- *expected value: $\mathbb{E}[B_H(t)] = 0$ for all $t \geq 0$;*
- *covariance function:*

$$\mathbb{E}[B_H(t)B_H(s)] = \frac{1}{2}\left(t^{2H} + s^{2H} - |t-s|^{2H}\right) \tag{2.1}$$

for all $t, s \geq 0$.

For any random variable associated with a stochastic process X, it is possible to define a corresponding characteristic function (CF). Specifically, for a stochastic process identified by a continuous probability density function (PDF) f_X, the

[1]The Hurst exponent is named after Harold Edwin Hurst (1880-1978), a British hydrologist who studied the long-term dependencies of water level fluctuations of the Nile River.

CF is given by:

$$\phi_X(\omega) = \mathbb{E}[e^{i\omega X}] = \int_{-\infty}^{+\infty} e^{i\omega x} f(x)\, dx \tag{2.2}$$

The description of a stochastic process is carried out through the determination of its statistical moments. Deriving the analytical expression of these moments involves calculating integrals that can be very complex. The characteristic function simplifies this calculation. Given a characteristic function ϕ_X, the k-th order moment is given by:

$$\mathbb{E}[X^k] = i^{-k} \left. \frac{d^k}{d\omega^k} \phi_X(\omega) \right|_{\omega=0} \tag{2.3}$$

In the case of a Gaussian process, such as fBM, it can be shown that the CF, and consequently all moments, are completely determined by the expected value $\mathbb{E}[X]$ and the variance of the process $\mathrm{Var}(X) = \mathbb{E}[X^2] - (\mathbb{E}[X])^2$. In particular, the CF takes the form:

$$\phi_X(\omega) = \mathbb{E}[e^{i\omega X}] = e^{i\mathbb{E}[X]\omega - \frac{1}{2}\mathrm{Var}(X)\omega^2} \tag{2.4}$$

Considering the definition of fractional Brownian motion, we can uniquely identify its characteristic function.
The fBM is a Gaussian stochastic process with random variables follow a Gaussian distribution: $X \equiv B_H(t) \sim \mathcal{N}(\mu, \sigma^2)$. To better specify the distribution, we must derive the mean μ and the variance σ^2. These are the two parameters required to identify the CF.

Proof. Since fBM is a central process, for all $t \geq 0$, its mean will be zero:

$$\mu \equiv \mathbb{E}[B_H(t)] = 0$$

Moreover, its variance can be deduced from the covariance function 2.1. Imposing $s = t$, we obtain the second moment:

$$\begin{aligned} \mathbb{E}[B_H^2(t)] &= \frac{1}{2}\left(t^{2H} + t^{2H} - |t-t|^{2H}\right) \\ &= \frac{1}{2} \cdot 2\, t^{2H} = t^{2H} \end{aligned}$$

Starting from the expression of the variance in terms of statistical moments, we get:

$$\sigma^2 \equiv \mathrm{Var}[B_H(t)] = \mathbb{E}[B_H^2(t)] - (\mathbb{E}[B_H(t)])^2 = t^{2H} - 0 = t^{2H}$$

The definition uniquely identifies the probability distribution followed by the process's random variable:

$$B_H(t) \sim \mathcal{N}(0, t^{2H}) \tag{2.5}$$

□

Remark 2.1. *For $H = 1/2$ the fractional Brownian motion coincides with the standard Brownian motion (BM). In this particular case:*

- *the mean remains zero:* $\mathbb{E}\left[B_{1/2}(t)\right] = 0$
- *the covariance function takes the typical expression of BM:*

$$\mathbb{E}\left[B_{1/2}(t)B_{1/2}(s)\right] = \frac{1}{2}\left(t + s - |t - s|\right) = \min(s, t) \overset{s\leq t}{=} s$$

- *the variance grows linearly with time:* $Var\left[B_{1/2}(t)\right] = t$.

At this point, it is possible to make the explicit form of the characteristic function of our process clear. Indeed, starting from the CF for a Gaussian process and substituting the values of μ and σ^2, we can write:

$$\phi_{B_H(t)}(\omega) = e^{-\frac{1}{2}t^{2H}\omega^2} \tag{2.6}$$

fBM Properties

The properties of fractional Brownian motion recall and generalize those of standard Brownian motion. The main properties of fBM are listed below.

1. fBM possesses the property of self-similarity. Specifically, it allows us to identify (in a distribution way) for all $a \in \mathbb{R}_+$

$$B_H(at) \sim a^H B_H(t) \tag{2.7}$$

Proof. The proof relies on the characteristic property of Gaussian processes being completely defined solely by their mean and their variance (or, in general, their covariance).
As a first step, we define a new Gaussian process: $X(t) \doteq a^{-H} B_H(at)$ with $a \in \mathbb{R}_+$. We now verify that this process is statistically identical to fBM by observing that the two share the same mean and covariance.

By the definition of fBM, its mean is zero, $\mathbb{E}[B_H(\tau)] = 0$ for all $\tau \geq 0$. Evaluating the expectation value of the process $X(t)$ for $t \geq 0$, we find that

this process is also centered:

$$\mathbb{E}[X(t)] = a^{-H}\mathbb{E}[B_H(at)] \overset{at\doteq\tau}{=} a^{-H}\mathbb{E}[B_H(\tau)] = 0$$

Analyzing the covariance of the defined process and recalling that of fBM 2.1, we obtain:

$$\begin{aligned}
\mathbb{E}[X(t)X(s)] &= \mathbb{E}\left[a^{-H}B_H(at)\cdot a^{-H}B_H(as)\right] \\
&= a^{-2H}\mathbb{E}[B_H(at)B_H(as)] \\
&= a^{-2H}\cdot\frac{1}{2}\left[(at)^{2H}+(as)^{2H}-|at-as|^{2H}\right] \\
&= a^{-2H}\cdot a^{2H}\frac{1}{2}\left[t^{2H}+s^{2H}-|t-s|^{2H}\right] \\
&= \mathbb{E}[B_H(t)B_H(s)]
\end{aligned}$$

Since the process $X(t)$ is a Gaussian process with the same mean and covariance as fBM, the two are statistically equivalent: $X(t) \sim B_H(t)$. We observe that multiplying by $a \in \mathbb{R}_+$:

$$\begin{aligned}
B_H(t) &\sim X(t) \\
a^H B_H(t) &\sim a^H X(t) \\
a^H B_H(t) &\sim a^H\left[a^{-H}B_H(at)\right] \\
a^H B_H(t) &\sim B_H(at)
\end{aligned}$$

Consequently, $B_H(at) \sim a^H B_H(t)$ holds for all $a \in \mathbb{R}_+$, which is our statement. □

Remark 2.2. *Note that for $H = 1/2$ we have $B_{1/2}(at) = a^{1/2}B_{1/2}(t)$, which is the self-similarity or scale-invariance property of BM, where the scaling relations are ($t \to at$, $x \to a^{1/2}x$).*

2. Due to the self-similarity property, the trajectories of $B_H(t)$ define a one-dimensional fractal with fractal (or Hausdorff) dimension $D = 2 - H$.

3. Almost surely (a.s.), meaning with probability one, the trajectories are continuous everywhere but nowhere differentiable.

4. A representation of fBM in terms of a stochastic integral, known as the

Mandelbrot-van Ness representation [9], can be defined as:

$$B_H(t) = B_H(0) + \frac{1}{\Gamma\left(H+\frac{1}{2}\right)}\left\{\int_{-\infty}^{0}\left[(t-s)^{H-\frac{1}{2}} - (-s)^{H-\frac{1}{2}}\right]\mathrm{d}W(s) + \int_{0}^{t}(t-s)^{H-\frac{1}{2}}\mathrm{d}W(s)\right\} \tag{2.8}$$

where Γ is the Gamma function, $W(s)$ is the Wiener process and $t > 0$ It is worth noting that this integral representation guarantees the mean and covariance of the process according to the fBM definition.

Remark 2.3. *The integral representation reproduces standard Brownian motion for $H = 1/2$.*
For this H value, the Gamma function is evaluated at 1, where $\Gamma(1) = 1$. Furthermore, the exponents inside the integrals become $\frac{1}{2} - \frac{1}{2} = 0$, consequently the integrands evaluate to unity:

$$B_{1/2}(t) = B_{1/2}(0) + \frac{1}{1}\left\{\int_{-\infty}^{0}[1-1]\,\mathrm{d}W(s) + \int_{0}^{t}1\,\mathrm{d}W(s)\right\}$$

The contribution of the long-term memory, indicated by the first integral, vanishes. The second integral remains, which allows us to identify the process with the BM, assuming the initial condition $B_{1/2}(0) = 0$:

$$B_{1/2}(t) = \int_{0}^{t}\mathrm{d}W(s) \equiv B(t)$$

2.2 Increments: Fractional Gaussian Noise and Autocorrelation

Definition 2.2. *Let $\{B_H(t) : t \geq 0\}$ be a trajectory of fractional Brownian motion; the increment over a time interval $[s,t]$ is defined as $\Delta B_H(s,t) \doteq B_H(t) - B_H(s)$.*

Since it is a linear combination of two Gaussian processes, the increment of fBm is itself a Gaussian process and is termed fractional Gaussian Noise (fGN). Remark that the analysis of individual increments plays a fundamental role in the study of fBM.

Below, recalling the properties of fBM, we examine and derive key properties of fGN.

fGN Properties

1. The fGN is a centred process and therefore has zero mean. This follows directly from being a combination of centred processes:

$$\mathbb{E}[\Delta B_H(s,t)] = \mathbb{E}[B_H(t)] - \mathbb{E}[B_H(s)] = 0 \tag{2.9}$$

2. Regarding the variance of fGN, taking into account the process's zero mean, we have:

$$\begin{aligned}
\mathrm{Var}[\Delta B_H(s,t)] &= \mathbb{E}[(\Delta B_H(s,t))^2] - (\mathbb{E}[\Delta B_H(s,t)])^2 \\
&= \mathbb{E}[(\Delta B_H(s,t))^2] \\
&= \mathbb{E}[(B_H(t) - B_H(s))^2] \\
&= \mathbb{E}[B_H^2(t)] + \mathbb{E}[B_H^2(s)] - 2\mathbb{E}[B_H(t)B_H(s)] \\
&= t^{2H} + s^{2H} - 2 \cdot \frac{1}{2}\left[t^{2H} + s^{2H} - |t-s|^{2H}\right] = |t-s|^{2H}
\end{aligned}$$

$$\mathrm{Var}[\Delta B_H(s,t)] = |t-s|^{2H} \tag{2.10}$$

   The variance of the increments depends exclusively on the duration of the time interval and is independent of absolute time.

3. Since fGN is a Gaussian process, its probability distribution is completely specified by its mean and variance:

$$\Delta B_H(s,t) \sim \mathcal{N}\left(0, |t-s|^{2H}\right) \tag{2.11}$$

4. We observe that the probability distribution function of fGN does not depend on absolute time, but only on the length of the time interval between the points of the fractional Brownian process. This indicates that, unlike fBM, the stochastic process of increments is stationary.

   The stationarity of the process $\Delta B_H(s,t)$ is demonstrated by verifying the invariance of its probability distribution function. For any time shift δ such that $t \to t+\delta$ and $s \to s+\delta$, the parameters identifying the PDF remain invariant:

$$\mathbb{E}[\Delta B_H(s+\delta, t+\delta)] = 0 = \mathbb{E}[\Delta B_H(s,t)]$$

$$\mathrm{Var}[\Delta B_H(s+\delta, t+\delta)] = |(t+\delta) - (s+\delta)|^{2H} = |t-s|^{2H} = \mathrm{Var}[\Delta B_H(s,t)]$$

Therefore, we can conclude that

$$\Delta B_H(s+\delta, t+\delta) \sim \Delta B_H(s,t) \tag{2.12}$$

proving that fGN is a stationary process. This property, which fractional Brownian motion lacks, makes working with increments far more practical when studying fractional Brownian processes.

Autocorrelation of Increments

In the literature, it is common to work with unit increments and to discretize the timeline using the time step $\Delta t = t - s$ between two values of fBM. Consequently, discrete time instances are denoted using a time index $n \in \mathbb{N}$ as $s = n\Delta t$ and $t = (n+1)\Delta t$.

Using the self-similarity 2.7 of fBm, a single increment can be expressed as:

$$X_t \doteq B_H((n+1)\Delta t) - B_H(n\Delta t) = [B_H(n+1) - B_H(n)]\,(\Delta t)^H \tag{2.13}$$

In this context, the mean and variance properties become:

- Mean: $\mathbb{E}[X_t] = \mathbb{E}[B_H(n+1)] - \mathbb{E}[B_H(n)] = 0$
- Variance: $\mathrm{Var}[X_t] = |(n+1) - n|^{2H} = 1$

We are now interested in deriving the covariance function between two increments separated by a time lag $\tau = k\Delta t$ with $k \in \mathbb{N}$.

Proof. For simplicity of calculation, we consider $\Delta t = 1$, which simplifies the notation. Using the definition of covariance and recalling that fGN is a centred process, we have:

$$\begin{aligned}
\gamma(k) &= \mathrm{Cov}(X_t, X_{t+k}) = \mathbb{E}[(X_t - \mu)(X_{t+k} - \mu)] = \mathbb{E}[X_t X_{t+k}] \\
&= \mathbb{E}\left[(B_H(n+1) - B_H(n))\,(B_H(n+k+1) - B_H(n+k))\right] \\
&= \mathbb{E}[B_H(n+1)B_H(n+k+1)] - \mathbb{E}[B_H(n+1)B_H(n+k)] \\
&\quad - \mathbb{E}[B_H(n)B_H(n+k+1)] + \mathbb{E}[B_H(n)B_H(n+k)]
\end{aligned}$$

Substituting the covariance function 2.1 from the definition of fBM, our expression

gives:

$$\begin{aligned}\gamma(k) = &\frac{1}{2}\left[(n+1)^{2H} + (n+k+1)^{2H} - |(n+1)-(n+k+1)|^{2H}\right] \\ &- \frac{1}{2}\left[(n+1)^{2H} + (n+k)^{2H} - |(n+1)-(n+k)|^{2H}\right] \\ &- \frac{1}{2}\left[n^{2H} + (n+k+1)^{2H} - |n-(n+k+1)|^{2H}\right] \\ &+ \frac{1}{2}\left[n^{2H} + (n+k)^{2H} - |n-(n+k)|^{2H}\right]\end{aligned}$$

Simplifying the algebraic steps yields the following result:

$$\gamma(k) = \frac{1}{2}\left[(k+1)^{2H} - 2k^{2H} + (k-1)^{2H}\right] \tag{2.14}$$

□

This demonstrates the independence of the covariance function from the specific time instances at which the increments are measured. It depends solely on the time lag k separating them.
Note that in this context, the definition of (auto-)covariance coincides with that of autocorrelation. Indeed, recalling that for $\Delta t = 1$ the variance of increments becomes equal to 1, we have:

$$\rho(k) = \frac{\mathrm{Cov}(X_t, X_{t+k})}{\sqrt{\mathrm{Var}(X_t) \cdot \mathrm{Var}(X_{t+k})}} = \gamma(k) \tag{2.15}$$

This property highlights the fact that increments of fBM are correlated, meaning that fBM is a non-Markovian meaning a process with memory, rapresented by H.

Remark 2.4. *In the case where $\Delta t \neq 1$, one can use the self-similarity property of fBM to understand how the result transforms. For a time lag of $k\Delta t$ between the two increments, we have:*

$$\begin{aligned}\gamma(k\Delta t) &= \mathbb{E}\left[(B_H((t+1)\Delta t) - B_H(t\Delta t))\,(B_H((t+k+1)\Delta t) - B_H((t+k)\Delta t))\right] \\ &= \mathbb{E}\left[(B_H(t+1) - B_H(t)) \cdot (\Delta t)^H\,(B_H(t+k+1) - B_H(t+k)) \cdot (\Delta t)^H\right] \\ &= \mathbb{E}\left[(B_H(t+1) - B_H(t))\,(B_H(t+k+1) - B_H(t+k))\right] \cdot (\Delta t)^{2H} \\ &= \gamma(k)(\Delta t)^{2H}\end{aligned}$$

To interpret H as a memory index, a long-range estimate of the covariance is commonly used in the literature. To this end, we calculate the covariance of the

increments $\gamma(k) = \mathbb{E}[X_0 X_k]$, where:

$$X_0 = B_H(1) - B_H(0) = B_H(1), \quad X_k = B_H(k+1) - B_H(k)$$

Expanding the product of the increments and using the covariance formula of fBM, we retrieve the difference between the following expected values:

$$\mathbb{E}[B_H(1)B_H(k+1)] = \frac{1}{2}\left[1^{2H} + (k+1)^{2H} - |1-(k+1)|^{2H}\right]$$
$$\mathbb{E}[B_H(1)B_H(k)] = \frac{1}{2}\left[1^{2H} + k^{2H} - |1-k|^{2H}\right]$$

Taking the difference, the covariance has the form:

$$\gamma(k) = \frac{1}{2}\left[(k+1)^{2H} - 2k^{2H} + (k-1)^{2H}\right]$$

At this point, we use the Taylor series expansion for the binomial term:

$$(1+x)^n \simeq 1 + nx + \frac{n(n-1)}{2!}x^2 + \frac{n(n-1)(n-2)}{3!}x^3 + o(x^3)$$

Note that for this expansion to hold, the condition $x \ll 1$ must be satisfied. In our case, for $k \gg 1$, we have the following two valid expansions:

$$(k+1)^{2H} = k^{2H}\left(1 + \frac{1}{k}\right)^{2H} = k^{2H}\left[1 + \frac{2H}{k} + \frac{2H(2H-1)}{2!}\frac{1}{k^2} + o(k^{-2})\right]$$
$$(k-1)^{2H} = k^{2H}\left(1 - \frac{1}{k}\right)^{2H} = k^{2H}\left[1 - \frac{2H}{k} + \frac{2H(2H-1)}{2!}\frac{1}{k^2} + o(k^{-2})\right]$$

Summing the two terms, we obtain:

$$(k+1)^{2H} + (k-1)^{2H} = k^{2H}\left[2 + \frac{2H(2H-1)}{k^2} + o(k^{-2})\right]$$

Approximating this result and substituting it into the calculated covariance, we finally obtain:

$$\gamma(k) \simeq \frac{1}{2}\left\{k^{2H}\left[2 + \frac{2H(2H-1)}{k^2}\right] - 2k^{2H}\right\}$$
$$= \frac{1}{2}\left[k^{2H}\frac{2H(2H-1)}{k^2}\right] \Rightarrow$$

$$\gamma(k) \simeq H(2H-1)k^{2H-2} \tag{2.16}$$

This result, depending solely on the time lag k and the Hurst index H, de-

scribes the long-range autocorrelation valid for $k \gg 1$. Furthermore, it exhibits a power-law structure. Note that:

- for $H > 1/2$, there is positive autocorrelation, $\gamma(k) > 0$;
- for $H < 1/2$, there is negative autocorrelation, $\gamma(k) < 0$;
- for $H = 1/2$, there is no correlation, $\gamma(k) = 0$ (moreover, since the increments are Gaussian processes, they are also independent of each other).

2.3 Fractional SDE and Generalized Fokker-Planck Equation

Fractional Stochastic Differential Equations

Fractional Brownian motion is a driftless stochastic process; hence, it is a process of pure diffusion. Identifying the infinitesimal increment of fBM as $\mathrm{d}B_H(t)$, the fractional Stochastic Differential Equation (fSDE) of the process is:

$$\mathrm{d}x(t) = \mathrm{d}B_H(t) \tag{2.17}$$

The meaning of this relation becomes explicit when formulated as an integral equation. Assuming standard initial conditions, $B_H(0) = 0$ and $x(0) = 0$ almost surely, we can integrate the equation pathwise:

$$\int_0^t \mathrm{d}x(t') = \int_0^t \mathrm{d}B_H(t') \implies x(t) = B_H(t)$$

Therefore, from a statistical standpoint, the moments of $x(t)$ and $B_H(t)$ coincide:

- Mean: $\mathbb{E}[x(t)] = \mathbb{E}[B_H(t)] = 0$
- Variance: $\mathrm{Var}[x(t)] = \mathrm{Var}[B_H(t)] = t^{2H}$
- Covariance: $\mathbb{E}[x(t)x(s)] = \mathbb{E}[B_H(t)B_H(s)] = \frac{1}{2}\left[t^{2H} + s^{2H} - |t-s|^{2H}\right]$

The moments can also be derived using Fractional Stochastic Calculus, which employs a generalization of the Itô integral known as the Wick-Itô-Skorohod integral [10]. For this integral, imposing appropriate assumptions on a function $f(x)$, the following property holds:

$$\mathbb{E}\left[\int_0^t f(x)\,\mathrm{d}B_H(x)\right] = 0 \tag{2.18}$$

- Using the above property, the mean is expressed as:

$$\mathbb{E}[x(t)] = \mathbb{E}\left[\int_0^t \mathrm{d}B_H(t')\right] = 0$$

- For the variance, we must instead use a general result known as the isometry theorem [11], which expresses the expected value of the product of two stochastic integrals as a Riemann-Liouville integral:

$$\mathbb{E}\left[\int f(u)\,\mathrm{d}B_H(u)\int g(v)\,\mathrm{d}B_H(v)\right] = H(2H-1)\iint f(u)g(v)|u-v|^{2H-2}\,\mathrm{d}u\,\mathrm{d}v \tag{2.19}$$

To apply this to our situation, we consider $f(u) = 1$ and $g(v) = 1$. Renaming the variables and the integration limits yields:

$$\mathbb{E}\left[\int_0^t \mathrm{d}B_H(t')\int_0^t \mathrm{d}B_H(s')\right] = H(2H-1)\int_0^t\int_0^t |t'-s'|^{2H-2}\,\mathrm{d}t'\,\mathrm{d}s'$$

To evaluate this, we can split the double integral or exploit symmetry. Let us focus on the integral over t':

$$\int_0^t\int_0^t |t'-s'|^{2H-2}\,\mathrm{d}t'\,\mathrm{d}s' = \int_0^t \mathrm{d}s'\int_0^t |t'-s'|^{2H-2}\,\mathrm{d}t'$$

Fixing s' and integrating with respect to t', taking care of the absolute value, we obtain:

$$\int_0^t |t'-s'|^{2H-2}\,\mathrm{d}t' = \frac{1}{2H-1}\left[(t-s')^{2H-1} + s'^{2H-1}\right]$$

Now, integrating with respect to s':

$$\begin{aligned}
&\int_0^t \frac{1}{2H-1}\left[(t-s')^{2H-1} + s'^{2H-1}\right]\mathrm{d}s' \\
&= \left[-\frac{1}{(2H-1)2H}(t-s')^{2H} + \frac{1}{(2H-1)2H}s'^{2H}\right]_0^t \\
&= \frac{t^{2H}+t^{2H}}{2H(2H-1)} = \frac{2t^{2H}}{2H(2H-1)} = \frac{t^{2H}}{H(2H-1)}
\end{aligned}$$

Substituting this result back into the formula yields the variance:

$$\mathrm{Var}[x(t)] = \mathbb{E}[B_H^2(t)] = \mathbb{E}\left[\int_0^t \mathrm{d}B_H(t')\int_0^t \mathrm{d}B_H(s')\right] = t^{2H} \tag{2.20}$$

Generalized Fokker-Planck Equation

The results obtained for the mean and variance of fractional Brownian motion can also be derived through the explicit form of the probability density function associated with $B_H(t)$. This PDF is the solution to the Generalized (or fractional) Fokker-Planck (FP) equation, which takes the form:

$$\frac{\partial p(x,t)}{\partial t} = D(t)\frac{\partial^2 p(x,t)}{\partial x^2} \tag{2.21}$$

where $D(t) \doteq Ht^{2H-1}$ is the anomalous diffusion coefficient, defined such that for $H = 1/2$, the standard FP equation of pure diffusion is recovered.

Solution of the Generalized Fokker-Planck Equation

We attempt to solve this equation using the Fourier method. Consider the following initial value problem:

$$\begin{cases} \partial_t p(x,t) = D(t)\partial_x^2 p(x,t) \\ p(x,t) \xrightarrow{t\to 0} p(x,0) \doteq \delta(x) \end{cases} \tag{2.22}$$

To solve the equation, we use the Fourier transform to move to momentum space k:

$$\hat{p}(k,t) = \int \mathrm{d}x\, e^{-ikx} p(x,t) \quad \text{and} \quad p(x,t) = \frac{1}{2\pi}\int \mathrm{d}k\, e^{ikx}\hat{p}(k,t)$$

We can rewrite the initial condition as:

$$p(x,0) = \frac{1}{2\pi}\int \mathrm{d}k\, e^{ikx}\hat{p}(k,0) = \delta(x) \implies \hat{p}(k,0) = 1$$

In k-space, applying ∂_t and ∂_x^2 to the density and substituting into the FP equation gives:

$$\partial_t \hat{p}(k,t) = -D(t)k^2\hat{p}(k,t)$$

Using the separation of variables, we obtain:

$$\frac{\mathrm{d}\hat{p}(k,t)}{\hat{p}(k,t)} = -D(t)k^2\,\mathrm{d}t$$

Integrating both sides and using the initial condition, we have:

$$\hat{p}(k,t) = \hat{p}(k,0)e^{-k^2\int_0^t D(t')\,\mathrm{d}t'} = e^{-k^2\int_0^t Ht'^{2H-1}\,\mathrm{d}t'} = e^{-\frac{k^2}{2}t^{2H}}$$

At this point, we perform the inverse Fourier transform to reconstruct $p(x,t)$:

$$p(x,t) = \frac{1}{2\pi}\int e^{ikx}e^{-\frac{k^2}{2}t^{2H}}\,\mathrm{d}k = \frac{1}{2\pi}\int e^{-\frac{k^2}{2}t^{2H}+ikx}\,\mathrm{d}k$$

This can be solved by completing the square in the argument of the exponential, reducing it to a Gaussian-type integral:

$$e^{-\frac{k^2}{2}t^{2H}+ikx} = e^{-\frac{t^{2H}}{2}\left[k-\frac{ix}{t^{2H}}\right]^2}e^{-\frac{x^2}{2t^{2H}}}$$

Redefining $k' \doteq k - \frac{ix}{t^{2H}}$ implies $\mathrm{d}k' = \mathrm{d}k$, so the integral above can be written as:

$$p(x,t) = \frac{1}{2\pi}e^{-\frac{x^2}{2t^{2H}}}\int_{-\infty}^{\infty} e^{-\frac{k'^2}{2}t^{2H}}\,\mathrm{d}k'$$

This is a standard Gaussian integral and its value is $\sqrt{\frac{2\pi}{t^{2H}}}$, thus we obtain the result:

$$p(x,t) = \frac{1}{\sqrt{2\pi t^{2H}}}e^{-\frac{x^2}{2t^{2H}}}$$

We have successfully, as expected, shown that the PDF is a Gaussian with zero mean and variance t^{2H}. Therefore, if we use the initial conditions $x(0) = 0 = B_H(0)$, the solution to the generalized FP equation provides the following probability density function for fBM:

$$p_{fBM}(x,t) = \frac{1}{\sqrt{2\pi\mathrm{Var}[B_H(t)]}}\exp\left\{\frac{-\left(x-\mathbb{E}[B_H(t)]\right)^2}{2\mathrm{Var}[B_H(t)]}\right\} \tag{2.23}$$

Moment Evolution Relations

As with the standard Fokker-Planck equations, it is possible to write evolution equations for the moments in the fractional case as well. Recall that in the standard case, the full FP equation is:

$$\partial_t p(x,t) = -\partial_x\left[a_1(x)p(x,t)\right] + \frac{1}{2}\partial_x^2[a_2(x)p(x,t)] \tag{2.24}$$

with the corresponding Itô SDE:

$$\mathrm{d}x(t) = a_1(x)\,\mathrm{d}t + \sqrt{a_2(x)}\,\mathrm{d}W(t) \tag{2.25}$$

For such equations holds the following scaling relations:

$$\begin{cases} \frac{\mathrm{d}}{\mathrm{d}t}\mathbb{E}[x(t)] & = \langle a_1(x)\rangle \\ \frac{\mathrm{d}}{\mathrm{d}t}\mathbb{E}[x^2(t)] & = 2\langle x a_1(x)\rangle + \langle a_2(x)\rangle \end{cases} \tag{2.26}$$

Proof. In the generalized context, the full standard FP equation takes the form:

$$\partial_t p(x,t) = -\partial_x \left[a_1(x)p(x,t)\right] + D(t)\partial_x^2[a_2(x)p(x,t)]$$

which corresponds to the following fractional SDE (under the Wick-Itô-Skorohod interpretation) [12]:

$$\mathrm{d}x(t) = a_1(x)\,\mathrm{d}t + \sqrt{a_2(x)}\,\mathrm{d}B_H(t)$$

In this case, the scaling relations become:

$$\begin{aligned} \frac{\mathrm{d}}{\mathrm{d}t}\mathbb{E}[x(t)] &= \langle a_1(x)\rangle \\ \frac{\mathrm{d}}{\mathrm{d}t}\mathbb{E}[x^2(t)] &= 2\langle x a_1(x)\rangle + 2D(t)\langle a_2(x)\rangle \end{aligned}$$

Let us prove the second relation:

$$\frac{\mathrm{d}}{\mathrm{d}t}\mathbb{E}[x^2(t)] = \frac{\mathrm{d}}{\mathrm{d}t}\int x^2 p(x,t)\,\mathrm{d}x = \int x^2 \partial_t p(x,t)\,\mathrm{d}x$$

Substituting the expression from the FP equation, we get:

$$\frac{\mathrm{d}}{\mathrm{d}t}\mathbb{E}[x^2(t)] = \underbrace{-\int x^2 \partial_x\left[a_1(x)p(x,t)\right]\mathrm{d}x}_{=\alpha} + \underbrace{D(t)\int x^2\partial_x^2[a_2(x)p(x,t)]\,\mathrm{d}x}_{=\beta}$$

This gives two integrals that can both be solved by parts: For the α term, we have:

$$-\int x^2\partial_x\left[a_1(x)p(x,t)\right]\mathrm{d}x = \underbrace{\left[-2xa_1(x)p\right]_{-\infty}^{+\infty}}_{=0} + 2\int_{-\infty}^{+\infty} x a_1(x)p\,\mathrm{d}x = 2\langle x a_1\rangle$$

For the β term, integrating by parts twice, we obtain:

$$\begin{aligned} D(t)\int x^2\partial_x^2[a_2(x)p(x,t)]\,\mathrm{d}x &= D(t)\left\{\underbrace{[2x\partial_x[a_2(x)p]]_{-\infty}^{+\infty}}_{=0} - \int_{-\infty}^{+\infty} 2x\partial_x[a_2(x)p]\,\mathrm{d}x\right\} \\ &= 2D(t)\left\{\underbrace{[-a_2(x)p]_{-\infty}^{+\infty}}_{=0} + \int_{-\infty}^{+\infty} a_2(x)p\,\mathrm{d}x\right\} \\ &= 2D(t)\langle a_2(x)\rangle \end{aligned}$$

Substituting the results obtained for the two terms yields exactly the desired equation. A similar derivation can be carried out to prove the first relation. □

If we now apply the scaling relations to the generalized FP equation of pure drift:

$$\partial_t p(x,t) = D(t)\partial_x^2 p(x,t)$$

where $a_1(x) = 0$ and $a_2(x) = 1$, and with the initial condition $x(0) = 0$, we obtain:

- $\frac{\mathrm{d}}{\mathrm{d}t}\mathbb{E}[x(t)] = 0 \implies \mathbb{E}[x(t)] = 0$
- $\frac{\mathrm{d}}{\mathrm{d}t}\mathbb{E}[x^2(t)] = 2D(t)$ in this case, integrating gives:

$$\mathbb{E}[x^2(t)] = 2\int_0^t D(t')\,\mathrm{d}t' = 2\int_0^t Ht'^{2H-1}\,\mathrm{d}t' = \frac{1}{2H}2Ht^{2H} = t^{2H}$$

These results are entirely consistent with those seen for fBM. Therefore, it is possible to use scaling relations to verify the results obtained through fractional calculus.

Self-Similarity Property

Using the explicit form of the probability distribution function $p(x,t)$ for fBM, we can verify its scale-invariance property. Applying the transformation ($t \to \hat{t} = at$, $x \to \hat{x} = a^H x$), the PDF becomes:

$$\begin{aligned} p(x,t) = \frac{1}{\sqrt{2\pi t^{2H}}}\exp\left\{-\frac{x^2}{2t^{2H}}\right\} \implies \\ \hat{p}(\hat{x},\hat{t}) = \frac{1}{\sqrt{2\pi a^{2H}t^{2H}}}\exp\left\{-\frac{a^{2H}x^2}{2a^{2H}t^{2H}}\right\} = a^{-H}p(x,t) \end{aligned}$$

In this way, the normalization is preserved:

$$\int \mathrm{d}\hat{x}\, \hat{p}(\hat{x}, \hat{t}) = \int \mathrm{d}x\, a^H \cdot a^{-H} p(x,t) = 1$$

This property generalizes the self-similarity of the Wiener process, which is recovered for $H = 1/2$.

Let us now formally prove via the cumulative distribution functions that:

$$B_H(at) \sim a^H B_H(t)$$

Proof. We define the cumulative distribution function as:

$$\mathrm{CDF}(x) \doteq P[x] = \int_{-\infty}^{x} \mathrm{d}x'\, p(x', t)$$

Thus, the probability of the fBm position being less than or equal to x at time t is:

$$P[B_H(t) \leq x] = \frac{1}{\sqrt{2\pi t^{2H}}} \int_{-\infty}^{x} \exp\left\{-\frac{u^2}{2t^{2H}}\right\} \mathrm{d}u$$

If we apply the self-similarity transformation described above, we have:

$$\begin{aligned} P[B_H(at) \leq x] &= \frac{1}{\sqrt{2\pi (at)^{2H}}} \int_{-\infty}^{x} \exp\left\{-\frac{u^2}{2(at)^{2H}}\right\} \mathrm{d}u \\ &= \frac{a^{-H}}{\sqrt{2\pi t^{2H}}} \int_{-\infty}^{x} \exp\left\{-\frac{(a^{-H}u)^2}{2t^{2H}}\right\} \mathrm{d}u \end{aligned}$$

It is now convenient to perform a coordinate substitution where $s = a^{-H}u$, implying $\mathrm{d}u = a^H \mathrm{d}s$. The upper limit of the integral becomes $s = a^{-H}x$ and:

$$\begin{aligned} P[B_H(at) \leq x] &= \frac{a^{-H}a^H}{\sqrt{2\pi t^{2H}}} \int_{-\infty}^{a^{-H}x} \exp\left\{-\frac{s^2}{2t^{2H}}\right\} \mathrm{d}s \\ &= P\left[B_H(t) \leq \frac{x}{a^H}\right] = P[a^H B_H(t) \leq x] \end{aligned}$$

In conclusion, by the uniqueness theorem for cumulative distribution functions, it follows that $B_H(at) \sim a^H B_H(t)$.

□

Chapter 3

Simulation of Fractional Brownian Motion

In this chapter, we implement the simulation of fractional Brownian motion (fBM) through various algorithms (Cholesky Decomposition, Hosking's Algorithm, and the Davies-Harte Method). We select the most efficient approach and verify several fundamental properties of fBM: the Hurst parameter H as a correlation index, the Gaussian nature of the process with a variance scaling as a power law of H, and the analytical expression of the autocorrelation of its increments.

3.1 Sample Paths for Fractional Gaussian Noise and Fractional Brownian Motion

While BM is a Markov process, fBM is not. This characteristic makes its simulation significantly more complex than its standard [13]. In fact, for BM, the increments between different time steps are independent; consequently, the value of the path at any given instant depends solely on the value assumed at the immediately preceding instant. This simplification no longer holds for fBM, where the increments are no longer independent, meaning that the value of the path at any given time depends on the values assumed at all previous instants.

Analysis of the Main Algorithms for fBM Simulation

The implementation of the simulation is performed using a series of algorithms well-known in the literature [14]. We will limit our focus to reviewing and listing the main characteristics of three of them, selecting the most efficient one for our future developments.

Direct Algorithm (Cholesky Decomposition)

The Cholesky algorithm is the simplest among those discussed, and it exploits the characteristic of fBM being a Gaussian process fully defined by its covariance matrix. The implementation of the algorithm consists of the following steps:

1. Construction of the covariance matrix Σ for the N desired time steps, starting from the theoretical covariance between any two instants:

$$\gamma_{fBM}(s,t) = \mathbb{E}[B_H(s)B_H(t)] = \frac{1}{2}\left(s^{2H} + t^{2H} - |s-t|^{2H}\right) \tag{3.1}$$

2. Calculation of the lower triangular matrix L through the Cholesky decomposition:

$$\Sigma = LL^T \tag{3.2}$$

3. Generation of a vector $\mathbf{z}$ with N components sampled from a standard normal distribution $\mathcal{N}(0,1)$;

4. Calculation of the path points as components of the vector:

$$\mathbf{b} = L\mathbf{z} \tag{3.3}$$

The Cholesky algorithm involves a high computational cost of $O(N^3)$, which makes it unsuitable for simulating a large number of paths.

Hosking's Algorithm

Hosking's algorithm is the application to fBM of a more general mathematical method used to generate stochastic processes. This method allows the generation of a time series through an iterative sequence starting from the specific theoretical autocorrelation function of the process. Unlike the Cholesky Decomposition, this method generates fractional Gaussian noise (fGN), from which the fBM is subsequently derived. The steps of the iteration include:

1. Calculation of the autocovariance for the fGN between two time steps separated by an integer lag k:

$$\gamma_{fGN}(k) = \mathbb{E}[X_H(t)X_H(t+k)] = \frac{1}{2}\left(|k+1|^{2H} - 2|k|^{2H} + |k-1|^{2H}\right) \tag{3.4}$$

2. Calculation of the new reflection coefficient $\phi_{n,n}$ and update of the previous coefficients $\phi_{n,j}$;

3. Update of the conditional variance v_n;

4. Generation of the new fGN increment through a linear combination of the previous increments, weighted by the newly calculated reflection coefficients, plus the addition of Z_{n+1} sampled from a standard normal distribution $\mathcal{N}(0,1)$ with a weight depending on v_n:

$$X_{n+1} = \left(\sum_{j=1}^{n} \phi_{n,j} X_{n+1-j} \right) + \sqrt{v_n} Z_{n+1} \tag{3.5}$$

Hosking's algorithm is slightly faster, having a computational cost of $O(N^2)$; however, it is still unsuitable for generating a large number of paths.

Davies-Harte Method

The Davies-Harte method [15] addresses the computational inefficiency of the Cholesky decomposition by exploiting the Fast Fourier Transform (FFT), which reduces the computational cost to $O(N \log N)$. Similar to Hosking's approach, this algorithm does not directly simulate the fBM, but rather its increments (fGN). It leverages the stationarity of the process, which structures the covariance matrix as a Toeplitz matrix—a matrix where all diagonals are constant. The steps of the algorithm are as follows:

1. Calculation of the fGN covariance matrix using (3.4).It has dimensions $N \times N$ for the N points of the path, and its embedding into a circulant matrix C of dimension $M \times M$ (with $M = 2N - 2$) where each row is a right shift of the preceding one;

2. A fundamental property of the circulant matrix C allows the eigenvalues to be derived by performing the discrete Fourier transform: $\lambda = \mathcal{F}(\mathbf{c})$ where $\mathbf{c}$ is the vector containing the elements of C's first row:

$$\mathbf{c} = [g_0, g_1, \ldots, g_{N-2}, g_{N-1}, g_{N-2}, \ldots, g_1] \tag{3.6}$$

3. Furthermore, a circulant matrix is diagonalized by the Fourier transform and can be expressed as $\mathcal{F} C \mathcal{F}^{-1} = \Lambda$, where $\mathcal{F}$ is the discrete Fourier transform matrix and Λ is the diagonal matrix of the eigenvalues. Consequently, C decomposes in a manner similar to the Cholesky method in the

frequency domain:

$$C = (\mathcal{F}^{-1}\sqrt{\Lambda})(\sqrt{\Lambda}\mathcal{F}) = (\mathcal{F}^{-1}\sqrt{\Lambda})(\mathcal{F}^{-1}\sqrt{\Lambda})^{\dagger} \tag{3.7}$$

4. In the frequency domain, a complex vector $\mathbf{z} = \mathbf{a} + i\mathbf{b}$ is generated, where $\mathbf{a}$ and $\mathbf{b}$ are vectors of dimension M whose components are sampled from a standard normal distribution $\mathcal{N}(0, 1)$;

5. Calculation of the fGN path vector via the inverse matrix of discret Fourier transform:

$$\mathbf{x} = (\mathcal{F}^{-1}\sqrt{\Lambda})\mathbf{z} \tag{3.8}$$

   Note that due to the circulant embedding, only the first N components will be independent;

6. Computation of the cumulative sum of the independent elements of the vector $\mathbf{x}$ in order to determine the path points of the fBM.

For the purposes of this thesis, we select this algorithm as the core tool for generating fBM in Python. The implemented code is provided below:

```
def davies_harte_fbm(T, N, H):
    """
    Generates fractional Brownian motion paths using the
       Davies-Harte method.
    """
    def gamma(k, H):
        return 0.5 * (np.abs(k - 1)**(2 * H) - 2 * np.abs(k)
           **(2 * H) + np.abs(k + 1)**(2 * H))

    # 1. Construction of the circulant vector (length M = 2*
       N - 2)
    M = 2 * (N - 1)
    g = np.array([gamma(k, H) for k in range(N)])
    c = np.concatenate([g, g[1:-1][::-1]])

    # 2. Eigenvalues computation via FFT
    # fft gives the output without the normalization so it
       is needed to divide by M
    lk = np.fft.fft(c).real / M # Normalized vector of fft
    lk = np.maximum(lk, 0) # Numerical safety check for non-
       negativity
```

```
17
18      # 3. Random vector generation in the frequency domain
19      a = np.random.normal(size=M)
20      b = np.random.normal(size=M)
21      wk = np.zeros(M, dtype=complex)
22
23      # DC and Nyquist frequencies are imposed to be real
24      wk[0] = np.sqrt(lk[0]) * a[0]
25      wk[N-1] = np.sqrt(lk[N-1]) * a[N-1]
26
27      # Other frequencies (Hermitian Symmetry)
28      idx = np.arange(1, N-1)
29      wk[idx] = np.sqrt(lk[idx]) * ((a[idx] + 1j * b[idx]) /
           np.sqrt(2))
30      wk[M-idx] = np.conj(wk[idx])
31
32      # 4. Inverse FFT to get raw fGN (with unitary variance)
33      # ifft norlamizes the output so it is needed to multiply
            by M
34      fGn_raw = np.fft.ifft(wk).real * M
35      fGn_raw = fGn_raw[:N]
36
37      # 5. Time scaling and cumulative sum
38      dt = T / N
39      fGn = fGn_raw * (dt**H)
40      fBm = np.cumsum(fGn)
41
42      # The path starts at zero
43      path = np.concatenate([[0], fBm])
44
45      return path
```

As a consistency check for the various algorithms, the figure compares the fBM paths generated with different Hurst parameters H using the three previously described methods.

Sample Paths of fGN and fBM

Using the Davies-Harte algorithm, it is possible to simulate the values of the fBM increments $X_H(k)$, effectively simulating the fractional Gaussian noise (fGN). In

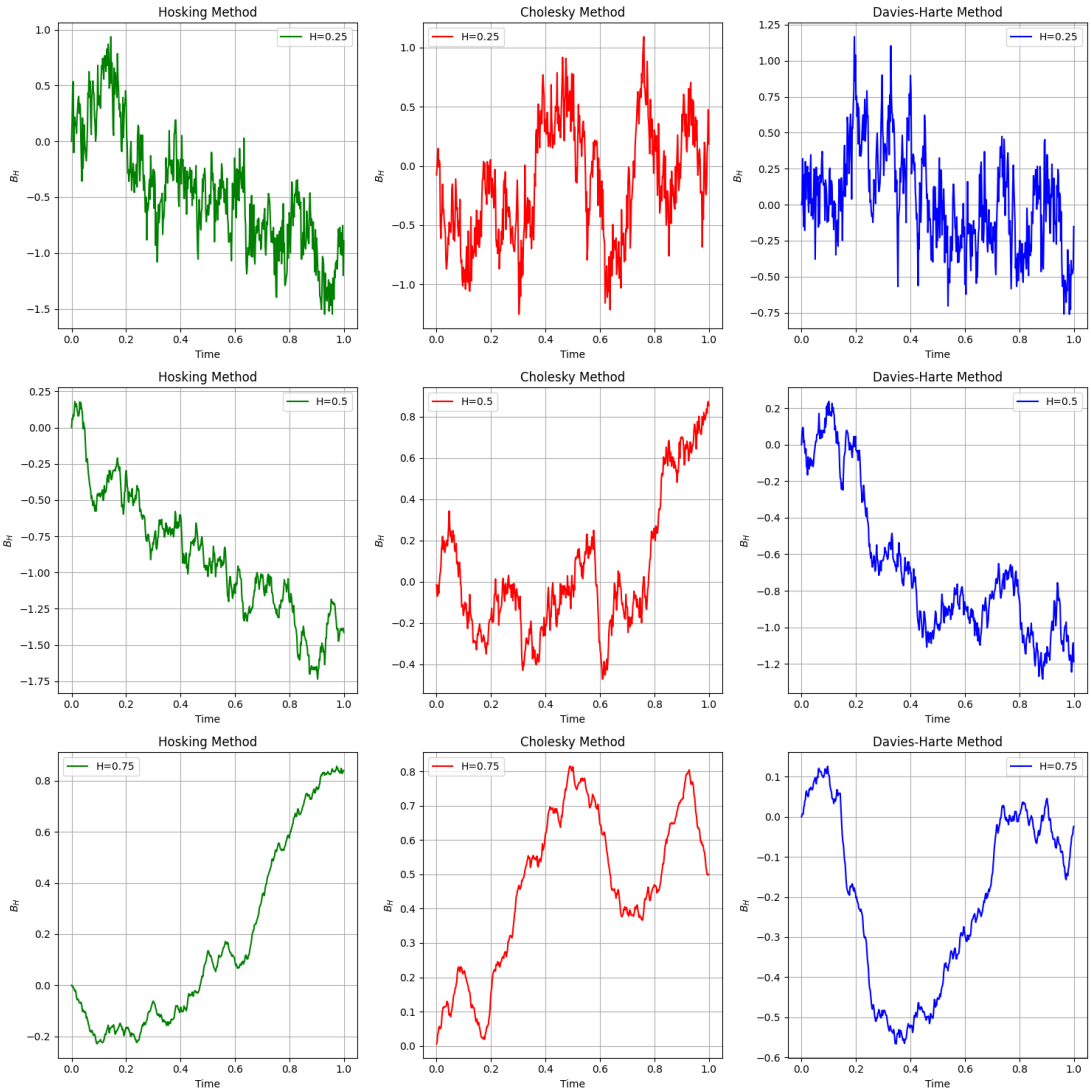

Figure 3.1: Comparison of fractional Brownian motion (fBM) simulation paths generated via Hosking, Cholesky, and Davies-Harte methods across different Hurst parameter values ($H = 0.25$, $H = 0.5$, and $H = 0.75$).

conducting this simulation, the objective was to observe the effect of the Hurst parameter H on the sample paths.

To this end, the simulation parameters were chosen to generate a unitary time step $\Delta t = 1$. This was enforced by setting a time horizon of amplitude $T = 10^3$ and a number of steps $N = 10^3$. Recalling that $\mathrm{Var}(X_H) = (\Delta t)^{2H}$, this configuration is particularly useful for maintaining a unitary variance that remains independent of H. Consequently, it allows for the isolated observation of the intrinsic effects of the fractional process.

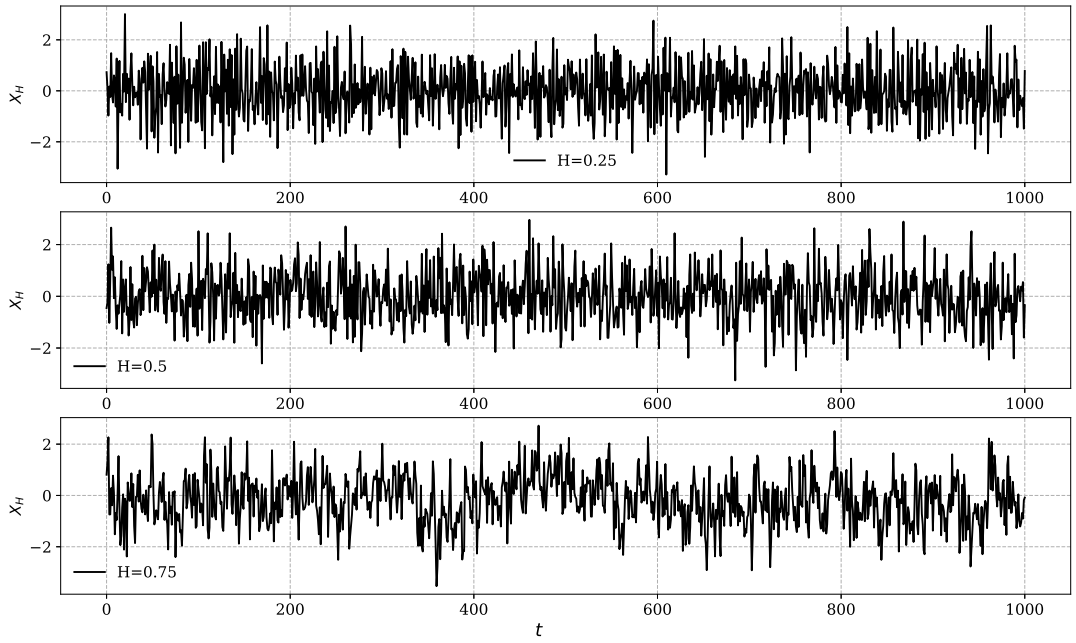

Figure 3.2: Simulation of Fractional Gaussian Noise (fGN) sample paths for different values of the Hurst parameter: $H = 0.25$ (anti-correlated), $H = 0.5$ (uncorrelated, corresponding to standard white noise), and $H = 0.75$ (correlated).

Observing the figure 3.2, the empirical variance appears to be unitary, precisely as anticipated. Investigating the effects of the Hurst parameter H, the following characteristics can be observed:

- For $H = 0.25$, the covariance between adjacent points is negative ($\gamma_{fGN}(1) < 0$) meaning that successive increments tend to be anti-correlated. Specifically, if an increment is above the mean (i.e., positive), the subsequent one will tend to be below the mean (i.e., negative). This behavior causes the fGN path to fluctuate rapidly, resulting in a visually more jagged or jagged graph;
- For $H = 0.5$, there is no covariance between adjacent points is ($\gamma_{fGN}(1) = 0$). This indicates the absence of correlation between neighboring points,

leading to independent increments and, consequently, to standard white noise;

- For $H = 0.75$, the covariance between adjacent points is positive ($\gamma_{fGN}(1) > 0$), implying that successive increments tend to be positively correlated and maintain their sign. This becomes visually evident as the graph exhibits distinct "valleys" and "hills", since the trajectories tend to move collectively upward or downward, creating the illusion of a trend. Nonetheless, both the variance and the mean calculated across all points remain identical to the previous cases.

The fGN provides a representation of the average velocity of our system across time intervals of $\Delta t = 1$. From this perspective, moving from velocity to position requires computing the cumulative sum of the increments, thereby yielding the fBM:

$$B_H(t) = \sum_{k=1}^{t} X_H(k) \tag{3.9}$$

Note: If we define the fGN as $X_H(k\Delta t) = B_H((k+1)\Delta t) - B_H(k\Delta t)$, then $X_H(k\Delta t)$ exhibits a variance that scales with $(\Delta t)^{2H}$. Conversely, if we use the standard fGN $X_H(k)$ with unitary variance, when constructing the fBM we must include a scaling factor and consequently, in analogy with standard Brownian Motion, we will write: $B_H(t) = \sum_{k=1}^{t} X_H(k)(\Delta t)^H$. In our specific framework, since $\Delta t = 1$, the two definitions coincide. However, we will generally adopte the former definition, used in the Python code where the fGN is already pre-scaled by the factor $(\Delta t)^H$.

Observing the figure 3.2, it is evident that an increase in H leads to a clear transformation in the behavior of the simulated trajectories. Specifically:

- For $H < \frac{1}{2}$, the negative correlations among the increments yield a rough sample path that exhibits a strong mean-reverting behavior, tending to remain close to its mean. Notably, in this specific simulation, the trajectory stays strictly confined within the $[-5, 5]$ interval;

- For $H = \frac{1}{2}$, the independent increments produce a sample path corresponding to a standard Brownian Motion, which is simply generated as $W(t) = \sum_{k=1}^{t} \xi_k \sqrt{\Delta t}$, where ξ_k represents standard Gaussian white noise drawn from $\mathcal{N}(0, 1)$. In this scenario, the trajectory does not follow any well-defined trend;

- For $H > \frac{1}{2}$, the positive correlations result in a considerably smoother sample path, highlights the process's tendency to maintain its current direction called persistence. This behavior translates into a significantly larger deviation from the mean compared to trajectories with lower H values.

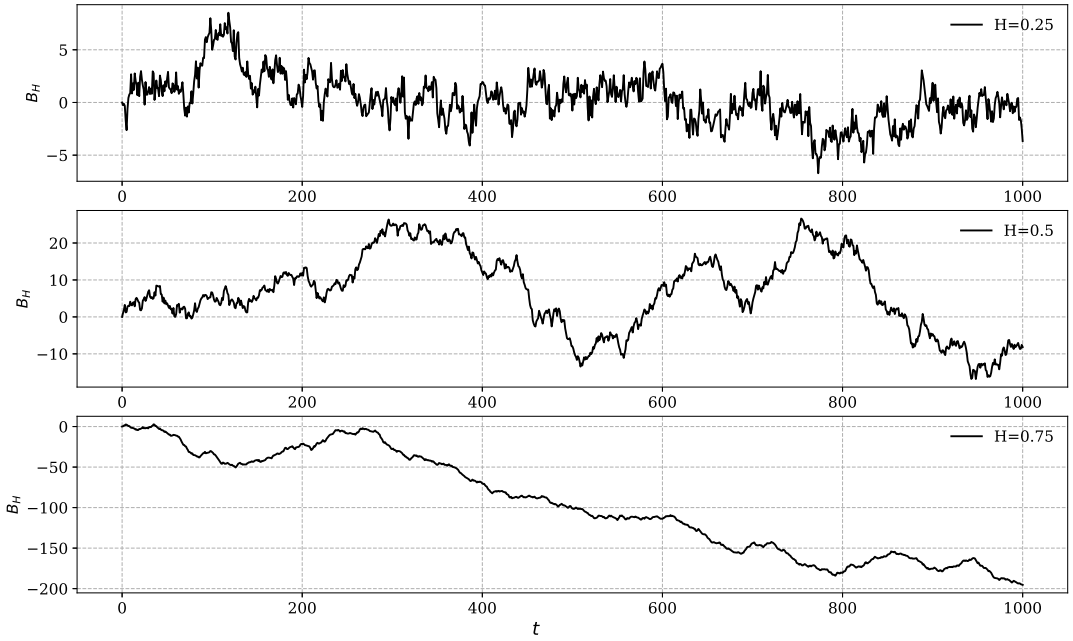

Figure 3.3: Simulation of Fractional Brownian Motion (fBM) sample paths obtained by cumulative summation of fGN increments for different Hurst parameter values: $H = 0.25$ (anti-persistent), $H = 0.5$ (standard Brownian motion), and $H = 0.75$ (persistent).

3.2 Sample Path Variance and Gaussian Distribution

To validate the implemented code, it is necessary to perform a comparison with the baseline model and verify its consistency. In practice, this entails utilizing the code to reproduce the fundamental theoretical properties of the fBM.

Sample Path Variance of fBM

The variance of the values assumed by the fBM sample paths is non-stationary and depends on the time according to $\mathrm{Var}(B_H(t)) = t^{2H}$.

To validate the code, one must verify this dependence on both H and time. Since computing the variance is an averaging operation, generating a large number

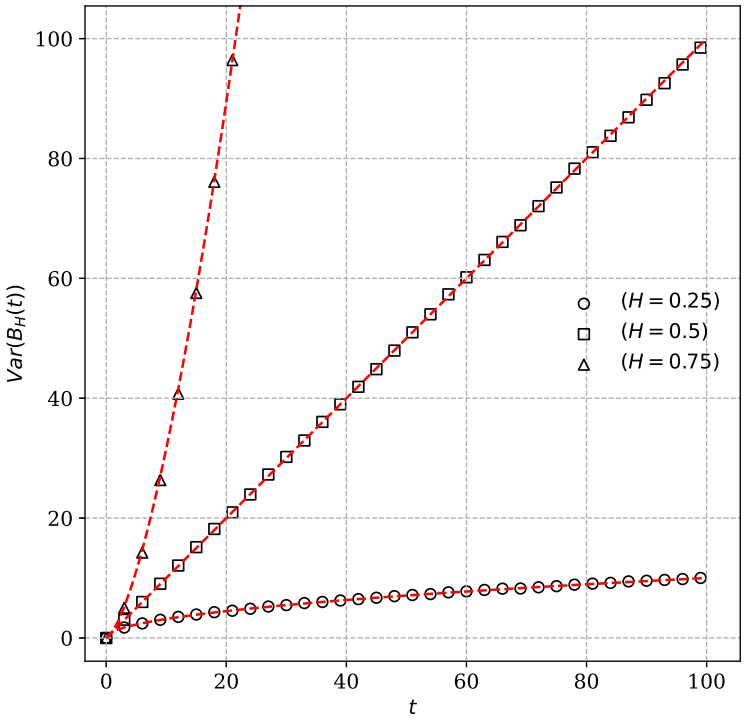

Figure 3.4: Temporal scaling of the fBM sample path variance $\mathrm{Var}(B_H(t))$ for different Hurst parameters ($H = 0.25$, $H = 0.5$, and $H = 0.75$). The discrete markers represent the empirical variance calculated over simulated trajectories, while the dashed red curves represent the theoretical power-law behavior.

of trajectories is required. In practice, $M = 10^4$ trajectories were simulated using the previously established parameters for T and N (which yield a time step $\Delta t = 1$). Subsequently, the variance is calculated for each step k across all trajectories according to:

$$\mathrm{Var}\{B_H(k\Delta t)\} = \frac{1}{M}\sum_{i=1}^{M} B_i^2(k\Delta t) \tag{3.10}$$

To verify the dependence on the Hurst parameter, this procedure is repeated for $H \in \{0.25, 0.5, 0.75\}$. Plotting the results yields the figure 3.4, which provides a direct comparison between the simulated data points and the theoretical curves. It can be observed that for $H = 0.5$, the variance is directly proportional to time, recovering the classic result of standard Brownian Motion where the "velocity" of system diffusion is constant. For other values of H, the process enters the regime of anomalous diffusion. Specifically:

- For $H < 0.5$, the fBM describes a sub-diffusive regime, in which the system's

expansion rate (i.e., the displacement from the initial position) slows down as time progresses;

- For $H > 0.5$, the fBM characterizes a super-diffusive regime, where the system's expansion rate accelerates over time.

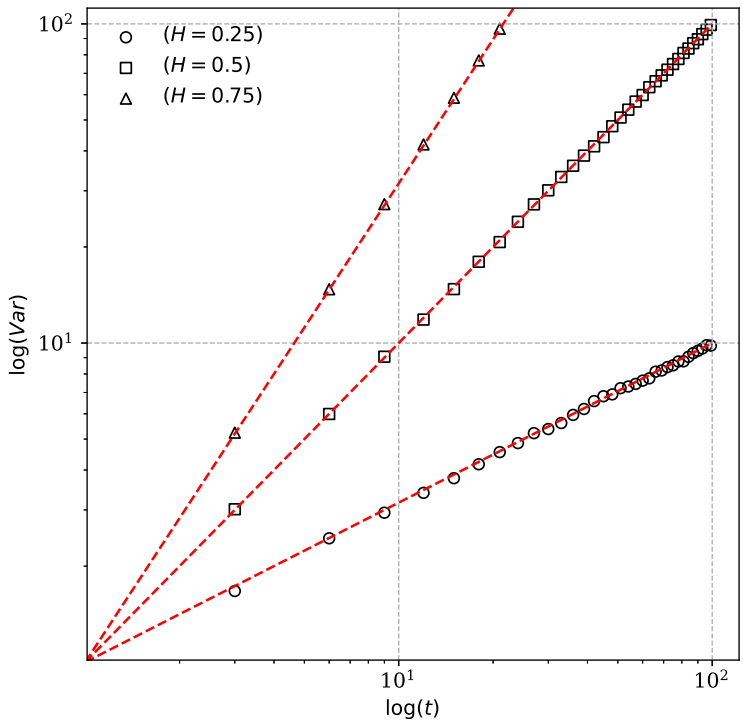

Figure 3.5: Log-log plot of the fBM sample path variance $\ln \mathrm{Var}(B_H(t))$ as a function of the elapsed time $\ln(t)$ for different Hurst parameters ($H = 0.25$, $H = 0.5$, and $H = 0.75$).

Furthermore, the self-similarity property of the fBM can be verified by analyzing the variance scaling on a log-log plot fig. 3.5, which transforms the power-law curves into straight lines. This self-similarity is evidenced by the fact that across different scales, the slope of each line remains constant and strictly dependent on H. Mathematically, taking the natural logarithm of the variance yields:

$$\mathrm{Var}\{B_H(t)\} = t^{2H} = e^{2H \ln t} \implies \ln \mathrm{Var}\{B_H(t)\} = 2H \ln t \tag{3.11}$$

Sample Path Distribution of fBM

Another fundamental property that can be verified is that the fBM is a Gaussian stochastic process. Specifically, the values assumed by the process at any given

instant of time are distributed according to a Gaussian distribution centered at 0, with a variance given by $\mathrm{Var}\{B_H(t)\} = t^{2H}$. Consequently, the bell-shaped probability density curves widen over time at a rate that strictly depends on the Hurst exponent H.

To verify that the implemented code satisfies this characteristic, M trajectories are simulated using the same parameters established previously. In this analysis, for each value of H, the values assumed by the process are sampled at three distinct time steps. Given that Δt is constant and the time is defined as $t = k\Delta t$, we select $k \in \{10, 50, 100\}$. For each chosen time instant, the simulated values of $B_H(k\Delta t)$ are utilized to construct an empirical histogram, which is then directly compared against the theoretical probability density function $p_{fBM}(x, t)$.

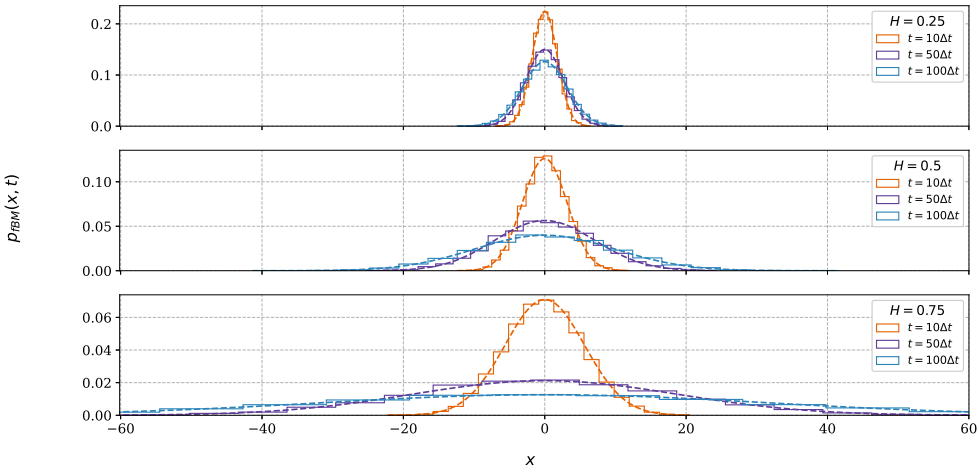

Figure 3.6: Empirical probability distribution of the fBM sample paths at different time steps ($t = 10\Delta t$, $t = 50\Delta t$, and $t = 100\Delta t$) for Hurst parameters $H = 0.25$, $H = 0.5$, and $H = 0.75$. The step-like histograms represent the simulated data sampled from $M = 10^4$ paths, while the dashed curves denote the corresponding theoretical Gaussian probability density functions $p_{fBM}(x, t)$.

In this manner, it is possible to confirm that the simulated process is indeed Gaussian and to observe how, at any identical time instant, the spread of the probability density curves strictly depends on the value of H. Compared to standard Brownian Motion ($H = 0.5$), the dispersion increases much more rapidly over time for $H > 0.5$. Conversely, for a given time horizon, the system with $H < 0.5$ exhibits a strong tendency to preserve its distribution scale or, at the very least, to experience a significantly slower expansion of its variance.

3.3 Autocorrelation of Increments

As a final analysis, we can verify that the implemented code correctly reproduces the theoretical autocorrelation of the fBM increments. Specifically, we investigate the asymptotic behavior for large time lags $\tau = k\Delta t \gg 1$, which is given by the theoretical expression:

$$\mathbb{E}\big\{B_H(\Delta t)[B_H(\tau) - B_H(\tau - \Delta t)]\big\} \simeq H(2H-1)\tau^{2H-2}(\Delta t)^2 \tag{3.12}$$

where the expectation value is computed over the products of the increments separated by a lag τ:

$$X_H(\Delta t) = B_H(\Delta t) - B_H(0) = B_H(\Delta t) \tag{3.13}$$

$$X_H(\tau) = B_H(\tau) - B_H(\tau - \Delta t) \tag{3.14}$$

By appropriately choosing the parameters to enforce $\Delta t = 1$ (specifically, setting $N = T = 128$ because the Davies-Harte algorithm is considerably faster when N is a power of 2), the expression simplifies significantly and depends solely on the discrete time lag k separating the two increments:

$$\mathbb{E}\big\{B_H(1)[B_H(k) - B_H(k-1)]\big\} \simeq H(2H-1)k^{2H-2} \tag{3.15}$$

Since the expectation value is an averaging operation, validating this expression requires generating a large number of simulations. In this framework, $M = 10^5$ trajectories were generated, and for each time step $k \in \{5, 10, 20, \ldots, 70, 80, 90, 100\}$, the empirical expectation is calculated as:

$$\mathbb{E}\big\{B_H(1)[B_H(k) - B_H(k-1)]\big\} = \frac{1}{M}\sum_{i=1}^{M}\Big\{B_H^i(1)\big[B_H^i(k) - B_H^i(k-1)\big]\Big\} \tag{3.16}$$

The figure 3.7 illustrates the simulated values compared against the theoretical curves for different values of H. It can be observed that for $H = 0.5$, the correlation is zero, consistent with the fact that $B_{0.5}(t)$ is a Wiener process characterized by independent increments. For $H < 0.5$, negative correlations are observed within the statistical error margins of the simulation in agreement with predictions. For $H > 0.5$, the correlations are positive and exhibit long-range dependence; indeed, a comparison with the results obtained for previous values of H reveals a significantly slower convergence rate. This behavior suggests the presence of long-term memory when the process enters a super-diffusive regime.

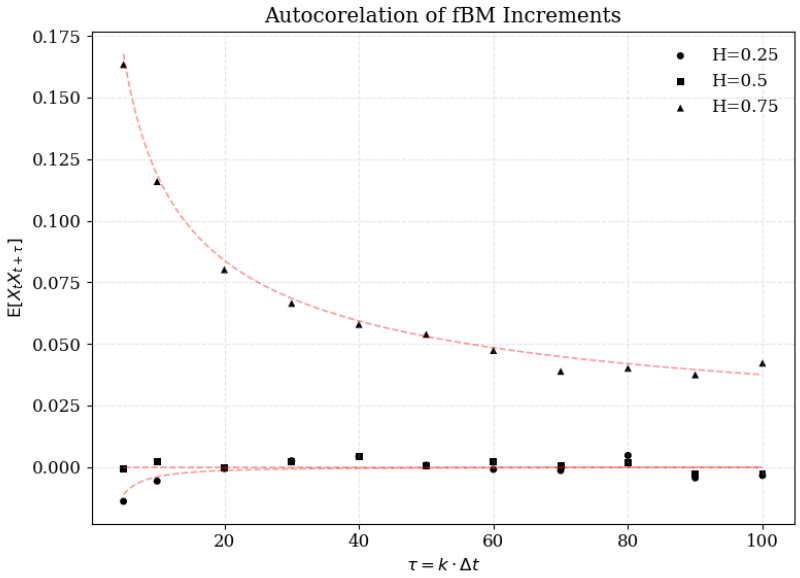

Figure 3.7: Asymptotic autocorrelation of fBM increments $\mathbb{E}[X_t X_{t+\tau}]$ as a function of the discrete time lag $\tau = k \cdot \Delta t$ for different Hurst parameters ($H = 0.25$, $H = 0.5$, and $H = 0.75$). The discrete markers represent the empirical expectation, while the dashed red lines denote the corresponding theoretical curves.

A further validation that can be performed using the long-range autocorrelation is to analyze the scaling on a log-log plot. In this framework, the theoretical power-law behavior is linearized, with the intercept and the slope depending exclusively on the Hurst parameter H:

$$\mathbb{E}\big\{B_H(1)[B_H(k) - B_H(k-1)]\big\} \simeq H(2H-1)e^{(2H-2)\ln k} \tag{3.17}$$

$$\Downarrow$$

$$\ln\Big(\mathbb{E}\big\{B_H(1)[B_H(k) - B_H(k-1)]\big\}\Big) \simeq \ln\big\{H(2H-1)\big\} + (2H-2)\ln k \tag{3.18}$$

To satisfy the domain of existence for the logarithm, H must take values strictly greater than 0.5; for this reason, the simulations were specifically executed for $H \in \{0.6, 0.7, 0.8, 0.9\}$.

The figure 3.8 demonstrates how the empirical data points align along the theoretical straight lines, validating the expected power-law correlation. A long-memory process is formally defined as one whose autocorrelation function decays sufficiently slowly such that its integral diverges. For this condition to hold within our framework, the absolute value of the power-law exponent must be less than or equal to 1, a requirement that is consistently satisfied for $H > 0.5$. In particular, this exponent (which corresponds to the H-dependent slope in our log-log plot)

quantifies the degree of memory inherent to the process. As H approaches 1, the generated lines tend to flatten, indicating an increasingly slower decay of the autocorrelation, which is consequently preserved over longer time horizons. This specific property enables the rigorous modeling of empirical phenomena characterized by positive long-range dependence.

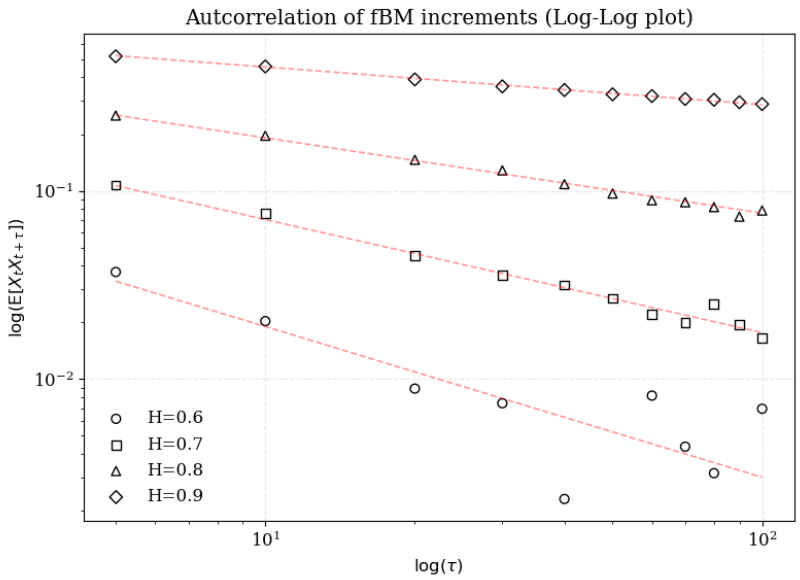

Figure 3.8: Log-log plot of the asymptotic autocorrelation of fBM increments $\ln(\mathbb{E}[X_t X_{t+\tau}])$ as a function of the time lag $\ln(\tau)$ for super-diffusive Hurst parameters ($H = 0.6, 0.7, 0.8$, and 0.9). The discrete markers represent the empirical scaling, while the dashed red lines illustrate the theoretical linearizations with slopes equal to $2H - 2$.

Chapter 4

Geometric Fractional Brownian Motion

In this chapter, we introduce geometric fractional Brownian motion (GfBM) to address the limitations of standard Brownian motion in financial modeling, incorporating anomalous long-range variance and the Hurst parameter into asset price dynamics. We then derive the analytical solutions for both standard geometric Brownian motion and its fractional extension evaluating their corresponding statistical moments. Next, we present numerical simulations generated via the to validate the theoretical properties, moments, and log-normal probability density functions across different Hurst exponents. The discussion concludes with the application of GfBM to the Fractional Black–Scholes model for option pricing and dynamic delta hedging, analyzing the impact of persistence on option evaluation.

4.1 Motivations

Standard Brownian motion (BM) fails to capture the complexity of financial time series. This provides the motivation for adopting fractional Brownian motion (fBM) in modeling asset price dynamics and in option pricing models [16].

The classic Black-Scholes-Merton model [17, 18]assumes that returns follow a Gaussian distribution with constant volatility and independent increments. However, the validity of this approach is challenged by empirical evidence, which reveals heavy-tailed distributions, volatility clustering, and long-range dependence; features that standard BM is unable to reproduce [19, 20, 21].

In this context, the generalized Hurst exponent (H) plays a central role, making it possible both to characterize the historical memory of processes and to distinguish the level of development of a market. Empirical studies on the Hurst

exponent show that financial markets exhibit different values depending on their degree of liquidity and maturity. In particular, emerging markets display persistent behaviour ($H > \frac{1}{2}$), whereas developed markets exhibit absence of memory or, to a lesser extent, anti-persistent behaviour ($H < \frac{1}{2}$). Therefore, in many cases, the stochastic nature of financial fluctuations deviates from the classical Samuelson model [22] based on standard BM ($H = \frac{1}{2}$) [23, 24, 21].

To incorporate the Hurst exponent for modelling long-range dependence in stochastic processes, it becomes necessary to generalize Samuelson's model [22] by introducing geometric fractional Brownian motion (GfBM), which uses fBM as its underlying process. However, the introduction of fBM presents non-trivial mathematical challenges, as this process is not a semimartingale for $H \neq \frac{1}{2}$ [19].

In this regard, the First Fundamental Theorem of Asset Pricing establishes the existence of an equivalent martingale measure as a necessary and sufficient condition for the absence of arbitrage; consequently, models driven by fBM theoretically allow for arbitrage opportunities.

Several solutions exist to guarantee the absence of arbitrage in fractional models. A first option, which is always viable, consists in restricting the class of admissible trading strategies. If, on the other hand, the goal is to eliminate arbitrage at its root, one can resort to calculus based on the Wick product–which, however, presents difficulties in assigning a concrete financial interpretation to the theory–or adopt models driven by two independent stochastic processes, one standard and one fractional, known as mixed models [25].

In this context, option pricing under the fBM assumption represents an active and constantly evolving area of research [19, 26]. Consequently, validating the algorithm requires a direct comparison between the theoretical model and numerical simulations. In particular, the Feynman-Kac formula, which establishes the connection between the fractional differential equation and its solution, allows for simulating the option price to be compared with the analytical solution. This comparison makes it possible to verify that numerical approximations maintain consistency with the solution obtained via fractional stochastic calculus.

Therefore, the implementation to be presented is not limited to a simple generalization of BM trajectories, but aims to demonstrate how integrating long-range memory into the Black-Scholes model allows for option price estimation and a risk management strategy more closely aligned with the reality of financial markets, whenever long-range dependence is observe [27].

4.2 Analytical Solution

Geometric Brownian Motion (GBM) is one of the most widely used stochastic processes in quantitative finance. Unlike standard Brownian Motion (BM), the value described by GBM is strictly positive. This makes it particularly suitable for modeling the time evolution of asset prices and, consequently, for serving as the core engine of the Black-Scholes-Merton model [17, 18] for option pricing. GBM is the process obtained as the solution to the following stochastic differential equation (SDE):

$$dS_t = \mu S_t \, dt + \sigma S_t \, dW(t) \tag{4.1}$$

where $W(t)$ denotes the Wiener process representing the BM.

To solve the SDE (4.1), both Itô and Stratonovich stochastic calculus are available. In this context, we will use Itô calculus. This ensures a zero expected value for the stochastic integral, making it preferable when aiming to guarantee the absence of arbitrage.

Within the framework of Itô calculus, the two terms constituting equation (4.1) are interpreted as follows:

- $\mu S_t \, dt$ is the drift term, which describes the mean of the stochastic process;
- $\sigma S_t \, dW(t)$ is the noise term and provides its variance.

The objective of our discussion is to employ fractional Brownian motion (fBM) to generalize and solve equation (4.1). By solving this generalized equation, we obtain a process known as fractional geometric Brownian motion (GfBM).

By introducing fBM into equation (4.1), we obtain a fractional Stochastic Differential Equation (fSDE):

$$dS_t = \mu S_t \, dt + \sigma S_t \, dB_H(t) \tag{4.2}$$

To obtain this equation, we replaced the Wiener process with fBM, denoted by $B_H(t)$, where H is the Hurst parameter. Note that, due to the properties of fBM, for $H = \frac{1}{2}$, equations (4.1) and (4.2) coincide. However, to preserve the interpretation of the terms constituting the equation, we require the Wick-Itô-Skorokhod (WIS) stochastic calculus described in [28]. This framework provides a fractional generalization of Itô calculus and ensures that the zero expected value property of the stochastic integral holds even for fractional processes:

$$\mathbb{E}\left[\int f(s) \, dB_H(s)\right] = 0 \tag{4.3}$$

In what follows, we will first address the case where the Hurst exponent is $H = \frac{1}{2}$, which reduces to the standard equation (4.1), and subsequently solve the fSDE (4.2) for $H \neq \frac{1}{2}$.

Solution for $H = \frac{1}{2}$

In this specific case, the process described by the fBM reduces to a Wiener process, such that $dB_{\frac{1}{2}}(t) = dW(t)$. The fSDE (4.2) thus reduces to the standard equation:

$$dS_t = \mu S_t\, dt + \sigma S_t\, dW(t) \quad \text{for } H = \frac{1}{2} \tag{4.4}$$

for which, as previously mentioned, Itô calculus applies.

A result of paramount importance that enables us to solve our problem is Itô's Lemma, which allows us to define the differential of a function $f = f(t, X_t)$ with continuous second derivatives, depending on a standard stochastic process X_t governed by $dX_t = a(X_t, t)\, dt + b(X_t, t)\, dW(t)$. It is expressed by the following formula:

$$\begin{aligned} df(X_t,t) = \left[\frac{\partial f(X_t,t)}{\partial t} + a(X_t,t)\frac{\partial f(X_t,t)}{\partial X_t} + \frac{1}{2}b^2(X_t,t)\frac{\partial^2 f(X_t,t)}{\partial X_t^2}\right] dt + \\ b(X_t,t)\frac{\partial f(X_t,t)}{\partial X_t} dW(t) \end{aligned} \tag{4.5}$$

Geometric Brownian Motion (GBM) is well suited for the application of this lemma. Considering the following identifications:

$$X_t \to S_t, \quad a(X_t, t) \to \mu S_t, \quad b(X_t, t) \to \sigma S_t$$

we can simplify our equation by applying the logarithmic transformation:

$$f(X_t, t) \to f(S_t) = \ln S_t$$

Computing the derivatives and substituting them into formula (4.5), the equation to be solved becomes:

$$d \ln S_t = \left(\mu - \frac{\sigma^2}{2}\right) dt + \sigma dW(t)$$

Integrating both sides over the interval $[0, t]$, setting $S(0) = S_0$ at $t = 0$, and

recalling that by definition $W(0) = 0$ almost surely, we have:

$$\int_{S_0}^{S_t} d\ln S_t' = \int_0^t \left(\mu - \frac{\sigma^2}{2}\right) dt' + \int_0^{W(t)} \sigma dW(t')$$

We thus obtain:

$$\ln\left(\frac{S_t}{S_0}\right) = \left(\mu - \frac{\sigma^2}{2}\right) t + \sigma W(t) \tag{4.6}$$

Note that the process governing the log-returns, i.e., the expression on the left-hand side of (4.6), is a BM with drift. As such, it follows a Gaussian probability distribution. Applying the exponential function to both sides and rearranging the terms yields the solution:

$$S_t = S_0 \exp\left(\left(\mu - \frac{\sigma^2}{2}\right) t + \sigma W(t)\right) \tag{4.7}$$

This solution represents the GBM and, being the exponential of a Gaussian process, its probability distribution is log-normal. This distribution guarantees the positivity of our stochastic variable, which is crucial as it ensures the validity of our model for describing asset prices and other commodities that must take strictly positive values.

Next, we proceed to compute the mean and variance from the statistical moments and correlation properties, first for the log-returns and subsequently for the asset prices themselves. As a first step, we analyze the log-returns described by equation (4.6).

- The mean is the expected value of the process:

$$\begin{aligned} \text{Mean} &= \mathbb{E}\left[\ln\left(\frac{S_t}{S_0}\right)\right] = \mathbb{E}\left[\left(\mu - \frac{\sigma^2}{2}\right) t + \sigma W(t)\right] \\ &= \left(\mu - \frac{\sigma^2}{2}\right) t + \sigma \mathbb{E}\left[W(t)\right] \\ &= \left(\mu - \frac{\sigma^2}{2}\right) t \end{aligned} \tag{4.8}$$

  In the last step, we exploited the zero-mean property of the BM. Furthermore, note that if we wished to obtain the expected value of $\ln S_t$ alone, an additional constant term would appear: $\mathbb{E}[\ln S_t] = \ln S_0 + \left(\mu - \frac{\sigma^2}{2}\right) t$

- The variance is calculated starting from the first two moments; hence, we

must compute the second moment:

$$\begin{aligned}\mathbb{E}\left[\ln^2\left(\frac{S_t}{S_0}\right)\right] &= \mathbb{E}\left[\left[\left(\mu-\frac{\sigma^2}{2}\right)t+\sigma W(t)\right]^2\right] \\ &= \mathbb{E}\left[\left(\mu-\frac{\sigma^2}{2}\right)^2 t^2 + 2\left(\mu-\frac{\sigma^2}{2}\right)\sigma t W(t) + \sigma^2 W^2(t)\right] \\ &= \left(\mu-\frac{\sigma^2}{2}\right)^2 t^2 + \sigma^2\mathbb{E}[W^2(t)] \\ &= \left(\mu-\frac{\sigma^2}{2}\right)^2 t^2 + \sigma^2 t\end{aligned}$$

In this calculation, besides the zero-mean property of the BM, we also accounted for the relation regarding its variance. Indeed, recall that:

$$\mathbb{E}[W^2(t)] - (\mathbb{E}[W(t)])^2 = \mathbb{E}[W^2(t)] = \mathrm{Var}[W(t)] = t$$

The variance of the log-returns is obtained from the moments as follows:

$$\begin{aligned}\text{Variance} = \mathrm{Var}\left[\ln\left(\frac{S_t}{S_0}\right)\right] &= \mathbb{E}\left[\ln^2\left(\frac{S_t}{S_0}\right)\right] - \mathbb{E}^2\left[\ln\left(\frac{S_t}{S_0}\right)\right] \\ &= \left(\mu-\frac{\sigma^2}{2}\right)^2 t^2 + \sigma^2 t - \left[\left(\mu-\frac{\sigma^2}{2}\right)t\right]^2 \\ &= \sigma^2 t \end{aligned} \tag{4.9}$$

- Log-returns show no autocorrelation. To verify this, equation (4.6) is integrated first over the interval $[t, t+\Delta t]$ and subsequently over $[t+\tau, t+\tau+\Delta t]$ with $\tau > 0$. This yields the following relations:

$$\begin{cases} \ln\left(\dfrac{S_{t+\Delta t}}{S_t}\right) = \left(\mu-\dfrac{\sigma^2}{2}\right)\Delta t + \sigma\Delta W(t) \\ \ln\left(\dfrac{S_{t+\tau+\Delta t}}{S_{t+\tau}}\right) = \left(\mu-\dfrac{\sigma^2}{2}\right)\Delta t + \sigma\Delta W(t+\tau) \end{cases} \tag{4.10}$$

where we have denoted the BM increments, also known as Wiener increments, by:

$$\Delta W(t) \doteq W(t+\Delta t) - W(t) \quad \text{and} \quad \Delta W(t+\tau) \doteq W(t+\tau+\Delta t) - W(t+\tau)$$

Recall that these increments have zero mean, $\mathbb{E}[\Delta W(t)] = 0$ for all $t > 0$,

and are independent, meaning:

$$\mathrm{Cov}(\Delta W(t), \Delta W(t+\tau)) = \mathbb{E}[\Delta W(t)\Delta W(t+\tau)] = 0$$

Computing the covariance between the two expressions in (4.10) using the mean and covariance properties of Wiener increments yields:

$$\begin{aligned}
&\mathrm{Cov}\left(\ln\left(\frac{S_{t+\Delta t}}{S_t}\right), \ln\left(\frac{S_{t+\tau+\Delta t}}{S_{t+\tau}}\right)\right) = \\
&\quad \mathbb{E}\left[\ln\left(\frac{S_{t+\Delta t}}{S_t}\right)\ln\left(\frac{S_{t+\tau+\Delta t}}{S_{t+\tau}}\right)\right] - \mathbb{E}\left[\ln\left(\frac{S_{t+\Delta t}}{S_t}\right)\right]\mathbb{E}\left[\ln\left(\frac{S_{t+\tau+\Delta t}}{S_{t+\tau}}\right)\right] \\
&\quad = 0
\end{aligned} \tag{4.11}$$

Next, we analyze the process describing the evolution of financial returns (4.7). To simplify the calculations, it is useful to note that we have two interdependent stochastic variables: a Gaussian variable describing the log-returns, $Z \doteq \ln S_t$, and a log-normal variable representing the financial returns, $Y \doteq e^Z = S_t$.

Our goal is to calculate the n-th moments of the log-normal variable. Note, however, that this is equivalent to the moment generating function (MGF) of the Gaussian distribution, which for $n \in \mathbb{N}$ is given by:

$$\mathbb{E}[Y^n] = \mathbb{E}[e^{nZ}] = M_Z(n) = e^{2n\mathbb{E}[Z] + \frac{1}{2}n^2\mathrm{Var}(Z)} \tag{4.12}$$

Using this expression and recalling the results previously obtained for the process describing log-returns, it is straightforward to determine the mean and variance of the GBM.

- The mean of the process is:

$$\begin{aligned}
\text{Mean} = \mathbb{E}[S_t] &= e^{\mathbb{E}[\ln S_t] + \frac{1}{2}\mathrm{Var}[\ln S_t]} \\
&= e^{\ln S_0 + \left(\mu - \frac{\sigma^2}{2}\right)t + \frac{1}{2}\sigma^2 t} \\
&= S_0 e^{\mu t}
\end{aligned} \tag{4.13}$$

- To compute the variance, we need the second moment:

$$\begin{aligned}\mathbb{E}[S_t^2] &= e^{2\mathbb{E}[\ln S_t]+2\mathrm{Var}[\ln S_t]} \\ &= e^{2\ln S_0+2\left(\mu-\frac{\sigma^2}{2}\right)t+2\sigma^2 t} \\ &= e^{\ln S_0^2+(2\mu+\sigma^2)t} \\ &= S_0^2 e^{(2\mu+\sigma^2)t} \end{aligned} \tag{4.14}$$

- The variance is therefore:

$$\begin{aligned}\text{Variance} = \mathrm{Var}[S_t] &= \mathbb{E}[S_t^2] - \mathbb{E}^2[S_t] \\ &= S_0^2 e^{(2\mu+\sigma^2)t} - S_0^2 e^{2\mu t} \\ &= S_0^2 e^{2\mu t}\left(e^{\sigma^2 t} - 1\right) \end{aligned} \tag{4.15}$$

Solution for $H \neq \frac{1}{2}$

Unlike the case where $H = \frac{1}{2}$, which reduces to a standard SDE, varying the Hurst parameter requires dealing with the general case of fractional SDEs:

$$dS_t = \mu S_t dt + \sigma S_t dB_H(t) \quad \text{for } H \neq \frac{1}{2} \tag{4.16}$$

In this setting, built upon a fractional process that possesses memory and is therefore not a martingale, one applies the rules of Wick-Itô-Skorokhod (WIS) calculus, where a formula analogous to the standard Itô formula holds [28].

Given a stochastic process defined by $dX_t^H = a(X_t^H, t)dt + b(X_t^H, t)dB_H(t)$, the expansion of a function $f = f(t, X_t^H) \in C^2$ is given by the fractional Itô Lemma, valid for all $H \in [0, 1]$:

$$\begin{aligned} f(X_t^H, t) = f(X_0^H, 0) &+ \int_0^t \frac{\partial f}{\partial s} ds + \int_0^t a \frac{\partial f}{\partial X_s^H} ds + \int_0^t b \frac{\partial f}{\partial X_s^H} dB_H(s) \\ &+ H \int_0^t s^{2H-1} b^2 \frac{\partial^2 f}{\partial (X_s^H)^2} ds \end{aligned} \tag{4.17}$$

where the last term arises from WIS calculus under the assumption that b is a linear function. This term accounts for the presence of "memory" and, for $H = \frac{1}{2}$, reduces to the characteristic term of the standard Itô formula: $\frac{1}{2}\int_0^t b^2 \frac{\partial^2 f}{\partial X_s^2} ds$.

Analogously to the previous derivation, we make the following substitutions:

$$X_t^H \to S_t, \quad a(X_t^H, t) \to \mu S_t, \quad b(X_t^H, t) \to \sigma S_t$$

Here again, we apply the logarithmic transformation to simplify the fSDE:

$$f(X_t^H, t) \to f(S_t) = \ln S_t$$

Computing the derivatives and substituting them into expression (4.17), we find that the log-returns are given by:

$$\begin{aligned}
\ln S_t &= \ln S_0 + \int_0^t \mu \, ds + \int_0^t \sigma \, dB_H(s) - H\sigma^2 \int_0^t s^{2H-1} \, ds \\
&= \ln S_0 + \mu t + \sigma B_H(t) - \frac{\sigma^2}{2} t^{2H} \\
&= \ln S_0 + \left[\mu t - \frac{\sigma^2}{2} t^{2H} \right] + \sigma B_H(t)
\end{aligned} \tag{4.18}$$

We observe that, as the first two terms are deterministic, the sole source of stochastic noise is provided by $B_H(t)$, which has a Gaussian PDF.

The defining properties of the process can be easily verified:

- Mean and variance are given by:

$$\text{Mean} = \mathbb{E}[\ln S_t] = \ln S_0 + \mu t - \frac{\sigma^2}{2} t^{2H} \tag{4.19}$$

$$\text{Variance} = \text{Var}[\ln S_t] = \sigma^2 t^{2H} \tag{4.20}$$

  Note that $\ln S_t$ is a linear combination of a Gaussian variable 4.18 and is therefore Gaussian itself. In particular, it is distributed as:

$$\ln S_t \sim \mathcal{N}\left(\ln S_0 + \mu t - \frac{\sigma^2}{2} t^{2H}, \, \sigma^2 t^{2H} \right)$$

- To compute the correlation of log-returns, for two time instants $t \neq s$, we first express the process as:

$$\begin{cases}
\ln S(t) = \ln S_0 + \left[\mu t - \dfrac{\sigma^2}{2} t^{2H} \right] + \sigma B_H(t) \\
\ln S(s) = \ln S_0 + \left[\mu s - \dfrac{\sigma^2}{2} s^{2H} \right] + \sigma B_H(s)
\end{cases} \tag{4.21}$$

  To compute the covariance between the two processes, we evaluate:

$$\begin{aligned}
\text{Cov}(\ln S(t), \ln S(s)) &= \sigma^2 \text{Cov}(B_H(t), B_H(s)) \\
&= \frac{\sigma^2}{2} \left(t^{2H} + s^{2H} - |t-s|^{2H} \right)
\end{aligned} \tag{4.22}$$

Exponentiating the log-returns expression 4.18 yields the formula for the GfBM, which describes the returns as log-normal stochastic variables:

$$S_t = S_0 \exp\left(\mu t - \frac{\sigma^2}{2} t^{2H} + \sigma B_H(t)\right) \tag{4.23}$$

This result is consistent with the literature [25, 29]. Since the process follows a log-normal distribution, we can use expression (4.12) to compute the moments and derive the mean and variance.

- For the mean, we have:

$$\begin{aligned} \text{Mean} = \mathbb{E}[S_t] &= e^{\mathbb{E}[\ln S_t] + \frac{1}{2}\text{Var}[\ln S_t]} \\ &= e^{\ln S_0 + \mu t - \frac{\sigma^2}{2} t^{2H} + \frac{1}{2}\sigma^2 t^{2H}} \\ &= S_0 e^{\mu t} \end{aligned} \tag{4.24}$$

  This result is identical to the one obtained for the standard GBM.

- For the variance, we first compute the second moment:

$$\begin{aligned} \mathbb{E}[S_t^2] &= e^{2\mathbb{E}[\ln S_t] + 2\text{Var}[\ln S_t]} \\ &= e^{2\ln S_0 + 2\mu t - \sigma^2 t^{2H} + 2\sigma^2 t^{2H}} \\ &= e^{\ln S_0^2 + 2\mu t + \sigma^2 t^{2H}} \\ &= S_0^2 e^{2\mu t + \sigma^2 t^{2H}} \end{aligned} \tag{4.25}$$

  from which we then obtain the variance:

$$\begin{aligned} \text{Variance} = \text{Var}[S_t] &= \mathbb{E}[S_t^2] - \mathbb{E}^2[S_t] \\ &= S_0^2 e^{2\mu t + \sigma^2 t^{2H}} - S_0^2 e^{2\mu t} \\ &= S_0^2 e^{2\mu t}\left(e^{\sigma^2 t^{2H}} - 1\right) \end{aligned} \tag{4.26}$$

4.3 Simulation of GfBM

In this section, the goal is to present the results of the simulation-based verification of the theoretical properties of the GfBM discussed in Section 4.2. The process is described by the stochastic differential equation:

$$dS = \mu S\, dt + \sigma S\, dB_H(t)$$

For the generation of the fBM, the Davies-Harte algorithm—extensively described in Chapter 3—was used, setting the input parameters to $T = 128$ and $N = 128$, which represent the time horizon and the total number of steps, respectively. These values were chosen to yield a unit time step $\Delta t = 1$. Within the simulation, to minimize the statistical error, the averaging operation was performed over $M = 10^4$ trajectories.

Below are presented the results obtained for two different values of the Hurst parameter: $H = 0.5$ and $H = 0.6$.

$H = 0.5$

In the case where $H = 0.5$, as discussed in the previous section, the elementary process reduces to standard Brownian motion (BM), and the overall model describes a geometric Brownian motion (GBM). The equation implemented to simulate this process corresponds to its exact analytical solution 4.7:

$$S(t) = S_0 \exp\left(\left(\mu - \frac{\sigma^2}{2}\right) t + \sigma W(t)\right)$$

To validate the model, the process was simulated to analyze and describe its main statistical moments as well as the probability distribution.

Statistical Moments

The theoretical expressions for the moments were verified by comparing the empirical results, obtained by averaging the simulated trajectories of $S(t)$, with the formulation given by:

$$\mathbb{E}[S_t^n] = e^{n\mathbb{E}[\ln S_t] + \frac{n^2}{2}\mathrm{Var}[\ln S_t]}$$

These predictions are strongly confirmed by the computational model, as shown in the figure 4.1.

Probability Density Function

Furthermore, the probability density function of $S(t)$ was verified, demonstrating its correspondence to a log-normal distribution expressed by:

$$p_{\mathrm{GBM}}(S_t, t) = \frac{1}{\sqrt{2\pi\sigma^2 t} \cdot S_t} \exp\left(-\frac{\left[\ln(S_t/S_0) - \left(\mu - \frac{\sigma^2}{2}\right) t\right]^2}{2\sigma^2 t}\right) \tag{4.27}$$

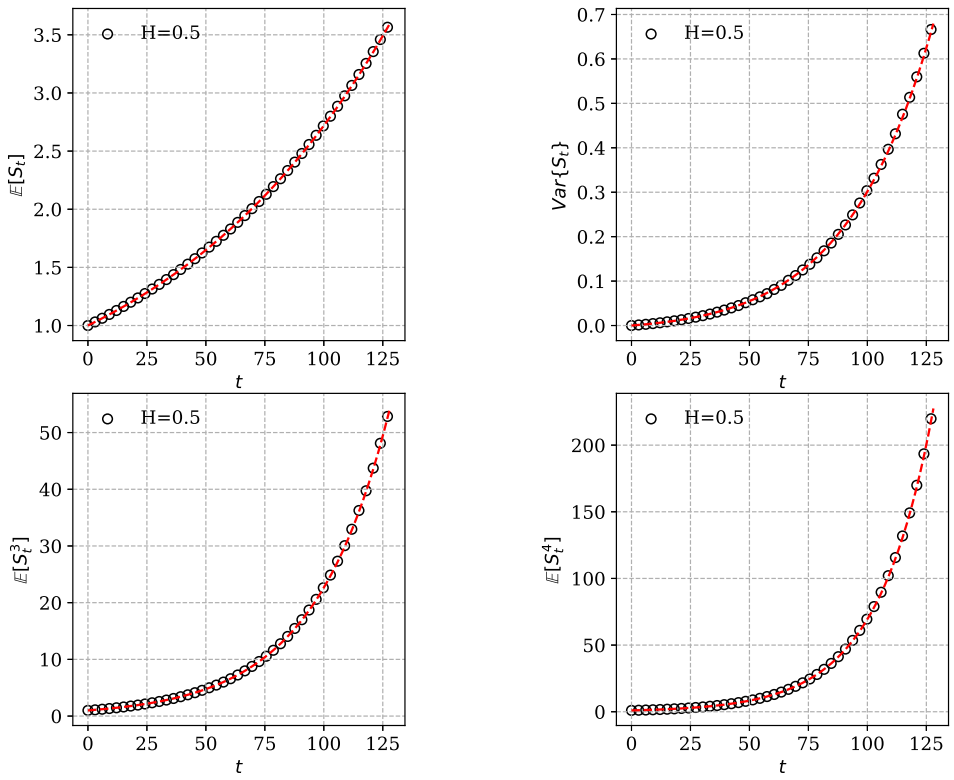

Figure 4.1: Comparison between theoretical statistical moments (red dashed line) and Monte Carlo simulation results (black circles) for $H = 0.5$ (standard geometric Brownian motion) over a time horizon $t \in [0, 128]$. The excellent agreement between the simulated points and theoretical curves across all analyzed moments validates the accuracy and convergence of the numerical implementation for $H = 0.5$.

This verification was performed by comparing the theoretical curve with the histograms constructed from the simulated values of $S(t)$ at three different time steps, $t \in \{10, 50, 100\}$, in order to highlight the temporal evolution of the PDF as well. The results are shown in Figure 4.2.

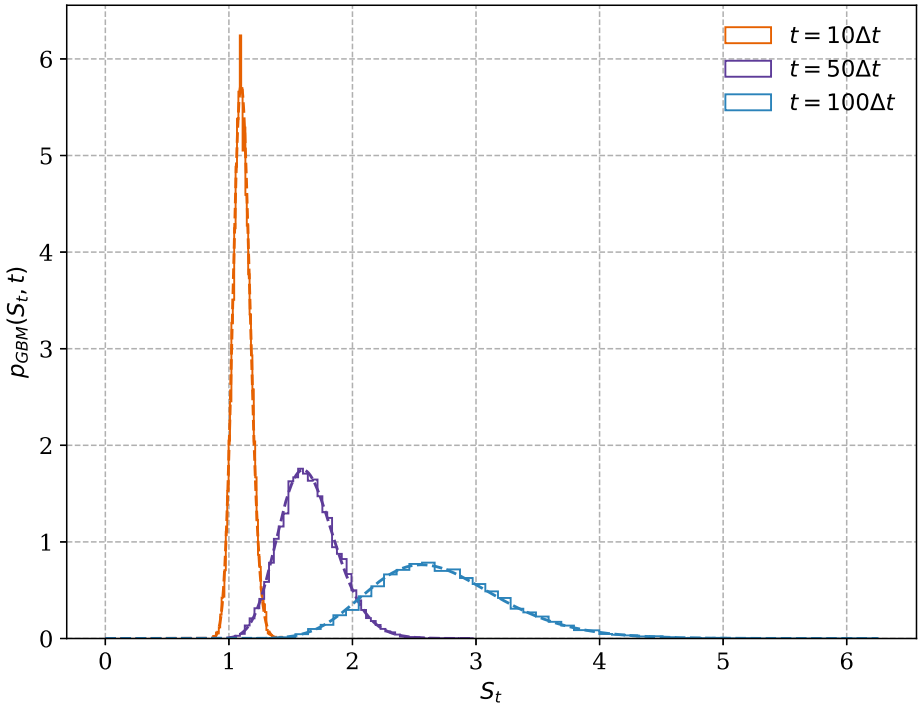

Figure 4.2: Probability density function $p_{\mathrm{GBM}}(S_t, t)$ for $H = 0.5$ evaluated at three distinct time steps ($t \in \{10\Delta t, 50\Delta t, 100\Delta t\}$). Empirical simulation histograms (step lines) are compared against the corresponding theoretical log-normal distributions (dashed lines).

The visual breakdown confirms key properties of the process:

- Mean shift: As time advances, the distribution shifts rightward, consistent with the growth of the expected value $\mathbb{E}[S_t]$.
- Dispersion growth: The profile broadens significantly, reflecting the exponential increase of the variance $\mathrm{Var}\{S_t\}$ over time.
- Peak decay: The maximum probability density value decreases steadily to maintain a total area under the curve equal to one.
- The high degree of alignment between the theoretical continuous curves and the numerical histograms validates the performance of the simulation

framework under the classic Black-Scholes-Merton model.

$H = 0.6$

Regarding the case where $H = 0.6$, the noise is driven by Fractional Brownian Motion (fBM), and the process reduces to a Geometric Fractional Brownian Motion (fGBM). Solving the fSDE yields the following analytical solution, which is suitable for numerical simulation:

$$S(t) = S_0 \exp\left(\mu t - \frac{\sigma^2}{2} t^{2H} + \sigma B_H(t)\right) \tag{4.28}$$

As was done for the case $H = 0.5$, we numerically verify the consistency of the theoretical results by simulating the main statistical moments and the PDF.

Statistical Moments

In this case as well, the values of the main moments obtained from the numerical simulation were compared with the theoretical results derived from the general formula. The resulting plots are reported in Figure 4.3.

A direct comparison with the standard case ($H = 0.5$, Figure 4.1) reveals two essential properties of the fractional process:

- Invariance of the expected value: The first moment $\mathbb{E}[S_t] = S_0 e^{\mu t}$ is completely independent of H, matching the exact trajectory of standard GBM.
- Amplification of higher-order moments: The variance and higher-order moments exhibit substantially faster growth over time. This behavior is governed by the t^{2H} dependence in the analytical moment equations.

The tight agreement between simulated points and theoretical curves confirms the accuracy of the numerical algorithm when handling persistent long-range dependencies.

Probability Density Function

In this case, the previously observed log-normal PDF is modified to incorporate the dependence on the Hurst parameter H:

$$p_{\text{fGBM}}(S_t, t) = \frac{1}{\sqrt{2\pi\sigma^2 t^{2H}} \cdot S_t} \exp\left(-\frac{\left[\ln(S_t/S_0) - \left(\mu t - \frac{\sigma^2}{2} t^{2H}\right)\right]^2}{2\sigma^2 t^{2H}}\right) \tag{4.29}$$

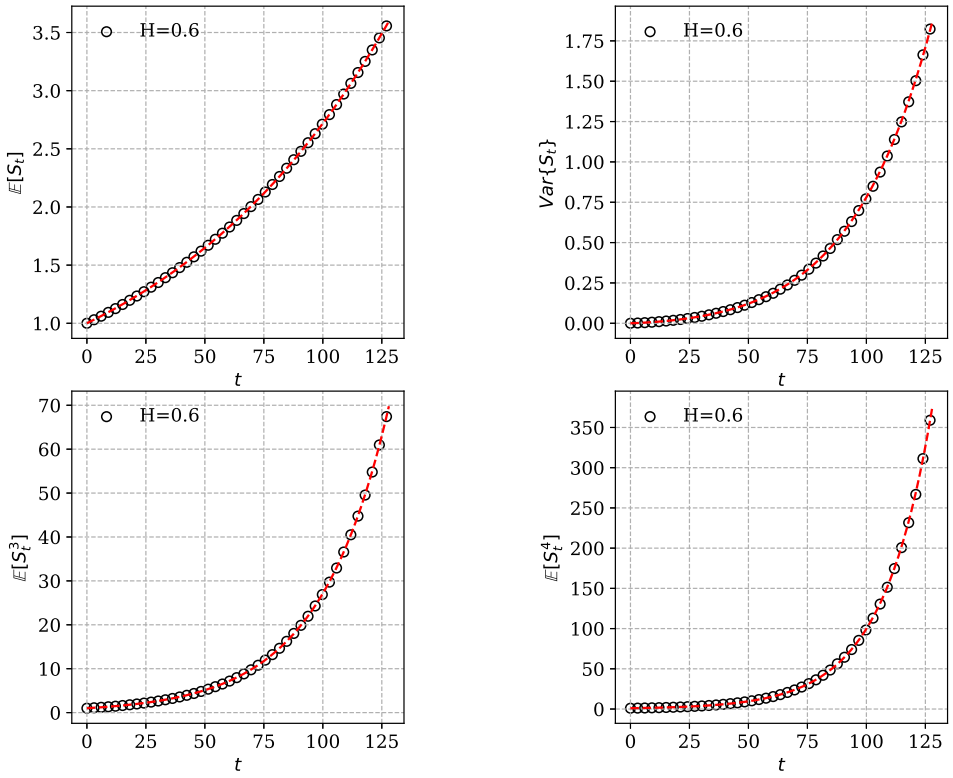

Figure 4.3: Comparison between theoretical statistical moments (red dashed line) and Monte Carlo simulation results (black circles) for $H = 0.6$ (Geometric Fractional Brownian Motion) over a time horizon $t \in [0, 128]$.

Performing a simulation analogous to the previous one with the same time parameters leads to the results condensed in Figure 4.4.

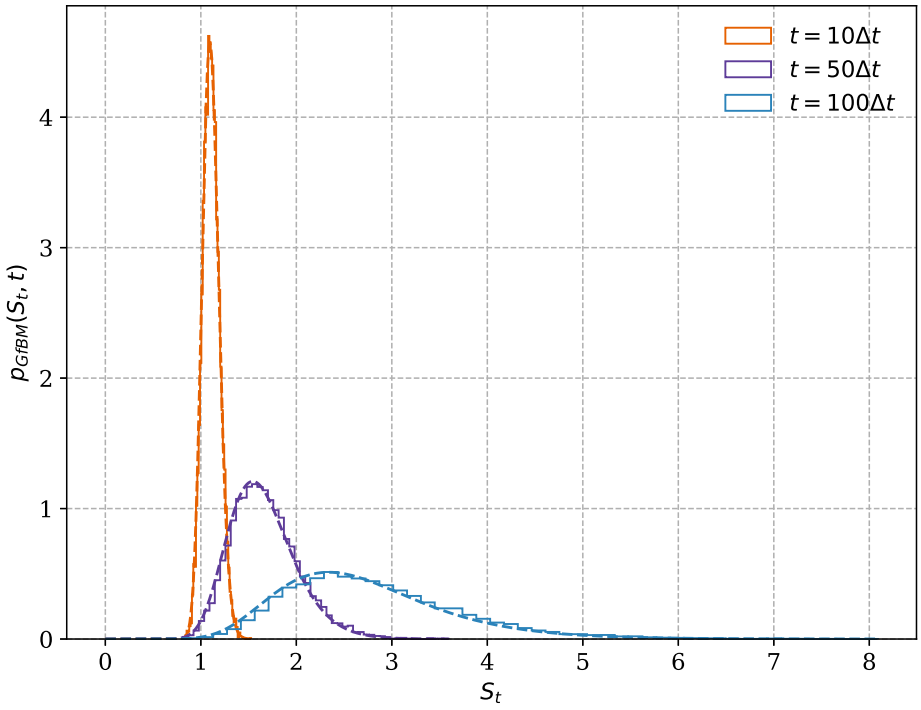

Figure 4.4: Probability density function $p_{\text{GfBM}}(S_t, t)$ for $H = 0.6$ (Geometric Fractional Brownian Motion) evaluated at three time steps ($t \in \{10\Delta t, 50\Delta t, 100\Delta t\}$). Empirical simulation histograms (step lines) are compared against theoretical fractional log-normal distributions (dashed lines).

Analyzing the graphs key differences emerge when comparing these results to the standard case ($H = 0.5$, Figure 4.2):

- Increased dispersion: Because the variance scales as t^{2H}, the probability distribution increases significantly faster, developing a heavier right tail.
- Lower peak probability: For any given time step, the maximum density value is lower.
- Preserved mean behavior: Despite the larger variance, the distribution remains centered around the same expected value as standard GBM.

Here too, strong agreement between the theoretical curves and simulation histograms confirms the reliability of the algorithm in reproducing fractional stochastic dynamics.

4.4 Fractional Black&Scholes Model

In this final section, the implemented model will be applied to validate and analyze the dynamics of financial options.

By employing Wick-Itô-Skorokhod (WIS) calculus, the Black-Scholes (BS) equation can be generalized to prices whose dynamics evolve according to the GfBM [29, 27]. Solving this equation [26], the price of a call option C, for the underlying asset price S at the current time t (*spot price*), is given by the following solution:

$$C(S,t) = SN(d_1) - Ke^{-r(T-t)}N(d_2) \tag{4.30}$$

where K represents the exercise price (*strike price*), r is the risk-free interest rate, and T denotes the expiration date (*maturity*). Denoting by $N(\cdot)$ the standard normal cumulative distribution function and by σ the volatility, the parameters d_1 and d_2 are given by:

$$d_1 = \frac{\ln\left(\frac{S}{K}\right) + r(T-t) + \frac{1}{2}\sigma^2(T^{2H} - t^{2H})}{\sigma\sqrt{T^{2H} - t^{2H}}} \tag{4.31}$$

$$d_2 = d_1 - \sigma\sqrt{T^{2H} - t^{2H}} \tag{4.32}$$

Note that the above equations, for $t = 0$ and $T = 1$, reproduce the solutions of standard Black-Scholes-Merton model [17, 18] for $H = \frac{1}{2}$. To simulate the call option price, we set the current time to $t = 0$, which implies taking the initial price of the underlying asset as $S(0) = S_0$. Under these initial conditions, the equations simplify as follows:

$$C(S_0,0) = S_0N(d_1) - Ke^{-rT}N(d_2) \tag{4.33}$$

$$d_1 = \frac{\ln\left(\frac{S_0}{K}\right) + rT + \frac{1}{2}\sigma^2T^{2H}}{\sigma T^H} \tag{4.34}$$

$$d_2 = d_1 - \sigma T^H \tag{4.35}$$

Remark 4.1. *In the fractional model, the solution to the Black-Scholes equation features a time dependence governed by the terms $T^{2H} - t^{2H}$, unlike the standard model where the dynamics depend solely on the time to maturity $(T - t)$. Consequently, the property of time-translation invariance no longer holds: the option price depends not only on the length of the time interval between the evaluation instant t and the expiration date T, but also on the absolute value of t itself. However, it is important to emphasize that the payoff function remains the same*

as in the classical model, namely,

$$\lim_{T^{2H}-t^{2H}\to 0} C(S,t) = \max(S-K,0)$$

Using this theoretical solution, we will evaluate the evolution of the option price C as a function of S_0 for $H \in \{0.5, 0.6, 0.7\}$, setting the following parameters: volatility $\sigma = 0.6$, risk-free rate $r = 0.05$, and strike price $K = 100$.

To test this theoretical behavior, we can exploit the dynamics of the GfBM via the Feynman-Kac formula, which in our context translates into simulating the discounted expected payoff:

$$C(S_0,0) = e^{-rT}\mathbb{E}[\max(S_T-K,0)] \sim e^{-rT}\frac{1}{M}\sum_{i=1}^{M}\max(S_T^i-K,0) \tag{4.36}$$

To describe the price evolution, we adopt the GfBM equation presented earlier:

$$S_T = S_0 e^{rT-\frac{\sigma^2}{2}T^{2H}+\sigma B_H(T)} \tag{4.37}$$

Operationally, for a given value of S_0, a trajectory of the fBM is simulated using the Davies-Harte method. The value of the trajectory at time $t = T$ is then extracted and inserted into the expression for $S(T)$, yielding the i-th realization S_T^i. By repeating this process $M = 10^2$ times and computing the Monte Carlo average prescribed by the Feynman-Kac formula, we obtain the numerical estimate of $C(S_0, 0)$. Finally, repeating this entire procedure for different values of S_0 across the domain of interest yields the simulated call option price curve as a function of the initial spot price, ready to be overlaid onto the theoretical curve.

For a maturity of $T = 0.5$, the performed simulations highlight the behaviors for the theoretical call option price, $C(S_0, 0)$, Figure 4.5 and for the call-option Delta, $\Delta = N(d_1)$, Figure 4.6.

The analysis of the results provides significant insights into the application of Geometric Fractional Brownian Motion for option pricing. The perfect alignment between the analytical solutions and the Monte Carlo validates the implemented numerical framework.

The figures illustrate the impact that memory has on pricing and hedging dynamics. From a financial perspective, introducing a Hurst parameter $H > 0.5$ describes a persistent market that tends to follow trends. For short time horizons ($T < 1$), this persistence reduces the unpredictability of the underlying asset.

Since an option's value is driven by uncertainty, lower variance translates into cheaper options, which explains the reduction in value of the call option price

observed in Figure 4.6.

This market memory also affects risk management. As shown in Figure 4.5, the Delta curve becomes more vertical. In this scenario, for the delta-hedging process any minor fluctuation of the underlying value near the strike price will generate grate increases in Delta value. Consequently, traders are forced to buy and sell much faster and more frequent in order to avoid risk exposures.

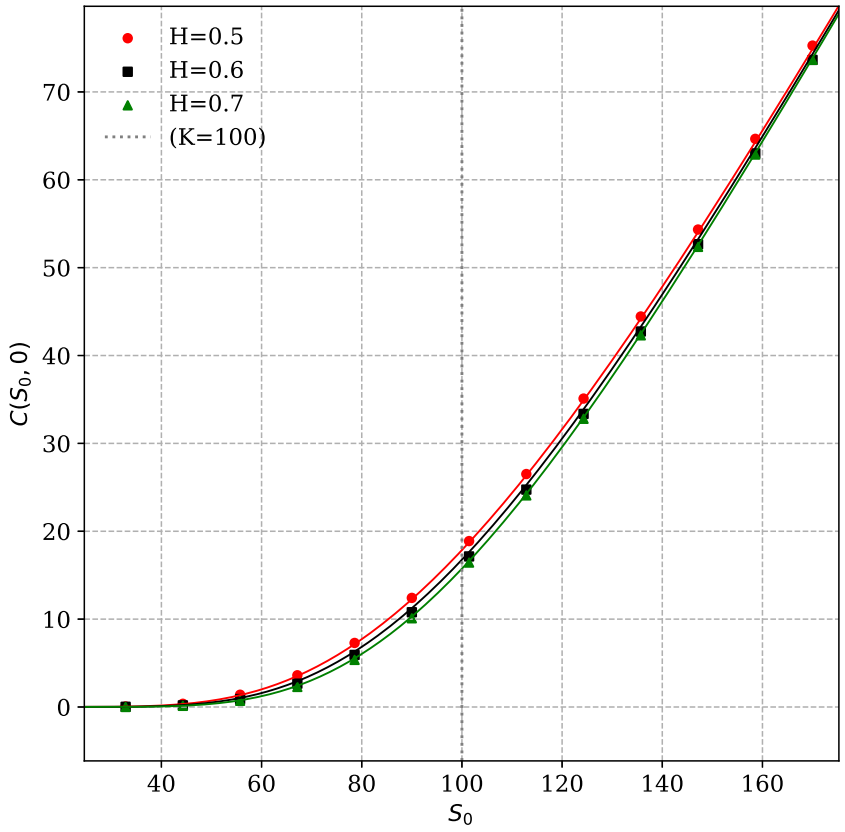

Figure 4.5: Call option price $C(S_0, 0)$ as a function of initial spot price S_0 for $H \in \{0.5, 0.6, 0.7\}$ with maturity $T = 0.5$, volatility $\sigma = 0.6$, risk-free rate $r = 0.05$, and strike price $K = 100$. Solid lines represent theoretical analytical solutions, whereas markers denote numerical Monte Carlo estimates via the Feynman-Kac formula.

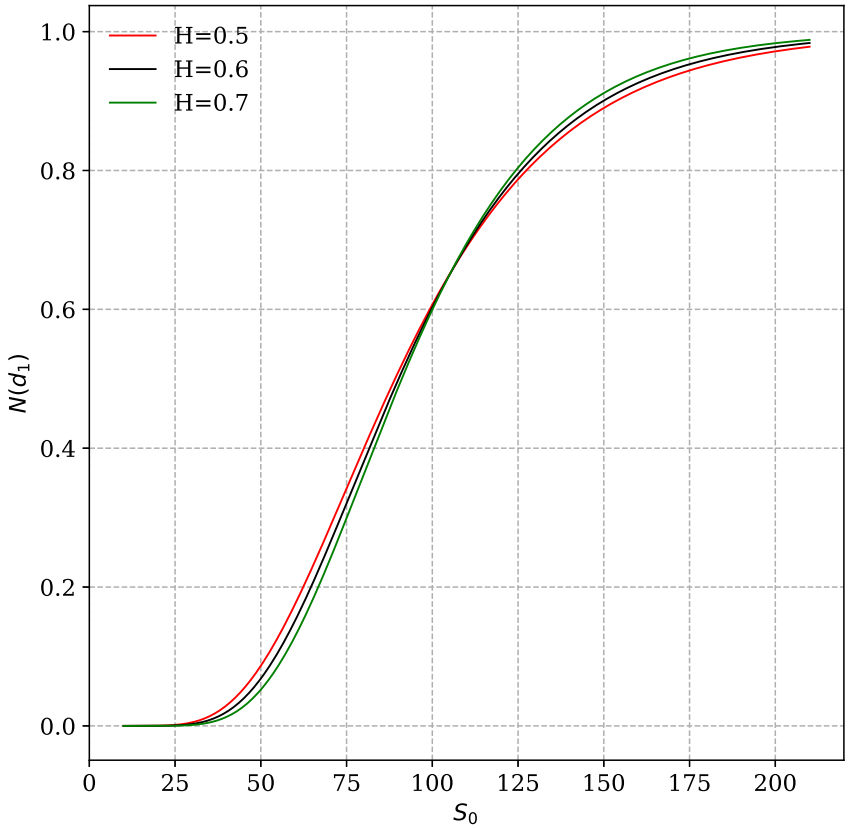

Figure 4.6: Theoretical Call option Delta, $\Delta = N(d_1)$, as a function of the initial spot price S_0 for $H \in \{0.5, 0.6, 0.7\}$ with maturity $T = 0.5$, volatility $\sigma = 0.6$, risk-free rate $r = 0.05$, and strike price $K = 100$.

Conclusion

The primary aim of this thesis was to numerically validate the statistical properties of fractional Brownian motion (fBM). Through the implementation of the Davies-Harte algorithm, favored over the Cholesky and Hosking methods for its computational efficiency, it was possible to generate a statistically significant sample of paths.

Numerical analyses performed on the simulations confirmed all theoretical aspects described by the mathematical model. In particular, the variance of the process demonstrated excellent agreement with the non-stationary power law t^{2H}, graphically validating the existence of anomalous diffusion regimes (sub-diffusive $H < 0.5$ and super-diffusive $H > 0.5$), both on a linear and via log-log scale. The Gaussian nature of the process was confirmed by the clear overlap between empirical histograms and theoretical probability density functions at various time instants. Finally, the long-range autocorrelation of the increments was verified, showing persistence for $H > 0.5$ and anti-persistence for $H < 0.5$, in agreement with the analytically predicted asymptotic decay.

A second objective of this thesis concerned the modeling and simulation of geometric fractional Brownian motion (GfBM), a process of fundamental importance in quantitative finance, used here to describe the stochastic evolution of financial returns. Using the formalism of Wick-Itô-Skorokhod (WIS) calculus, the analytical solution of the process was derived.

In this case as well, numerical simulations provided excellent confirmation of the expected theoretical properties. The comparison between generated sample paths and analytical results validated the behavior of statistical moments up to the fourth order. In particular, the invariance of the expected value with respect to the Hurst parameter was verified, alongside the clear amplification of the variance and higher-order moments. Analysis of the probability distributions confirmed the log-normal behavior of GfBM, displaying for $H = 0.6$ greater dispersion and a more pronounced tail compared to the standard Markovian case.

The final aim of this work was to apply GfBM to the pricing of financial

derivatives by generalizing the Black-Scholes model. Numerical validation of the analytical pricing formula was successfully performed using the Feynman-Kac representation, demonstrating excellent convergence between simulated outcomes and theoretical solutions.

The conducted analyses highlight crucial differences compared to the classical Black-Scholes model. Introducing a persistent Hurst parameter, consistent with the dynamics observed in emerging markets, results in a lower call option price compared to the classical model. Concurrently, the Delta sensitivity exhibits a steeper profile around the strike price, implying that minor fluctuations in the underlying asset price induce large price variations, thereby forcing market participants to execute faster and more frequent trades to hedge their risk.

In conclusion, the results of this thesis demonstrate that incorporating stochastic memory in a model yields greater fidelity to real-world market phenomenology, particularly in emerging markets or for equities where empirical evidence reveals long-range return dependencies.

Bibliography

[1] Louis Bachelier. "Théorie de la spéculation". In: *Annales scientifiques de l'École normale supérieure*. Vol. 17. 1900, pp. 21–86.

[2] Albert Einstein. "Über die von der molekularkinetischen Theorie der Wärme geforderte Bewegung von in ruhenden Flüssigkeiten suspendierten Teilchen". In: *Annalen der physik* 4 (1905).

[3] Paul Langevin et al. "Sur la théorie du mouvement brownien". In: *CR Acad. Sci. Paris* 146.530-533 (1908), p. 530.

[4] CW Gardiner. *Handbook of stochastic methods: for the natural and social sciences*. Springer, London, 2009.

[5] Hannes Risken. *Fokker-Planck equation: methods of solution and applications*. Springer, 1996.

[6] Norbert Wiener. "Differential-space". In: *Journal of Mathematics and Physics* 2.1-4 (1923), pp. 131–174.

[7] Bernt Oksendal. *Stochastic differential equations: an introduction with applications*. Springer Science & Business Media, 2013.

[8] Murad S Taqqu. "Benoıt Mandelbrot and fractional Brownian motion". In: *Statistical Science* (2013), pp. 131–134.

[9] Benoit B Mandelbrot and John W Van Ness. "Fractional Brownian motions, fractional noises and applications". In: *SIAM review* 10.4 (1968), pp. 422–437.

[10] Francesca Biagini et al. *Stochastic calculus for fractional Brownian motion and applications*. Springer, 2008.

[11] Tyrone E Duncan, Yaozhong Hu, and Bozenna Pasik-Duncan. "Stochastic calculus for fractional Brownian motion I. Theory". In: *SIAM Journal on Control and Optimization* 38.2 (2000), pp. 582–612.

[12] Yaozhong Hu and Bernt Øksendal. "Fractional white noise calculus and applications to finance". In: *Infinite dimensional analysis, quantum probability and related topics* 6.01 (2003), pp. 1–32.

[13] Georgiy Shevchenko. "Fractional Brownian motion in a nutshell". In: *arXiv preprint arXiv:1406.1956* (2014).

[14] Zijie Feng. *Stock-price modeling by the geometric fractional Brownian motion: A view towards the Chinese financial market*. 2018.

[15] Robert B Davies and David S Harte. "Tests for Hurst effect". In: *Biometrika* 74.1 (1987), pp. 95–101.

[16] Wolfgang Paul and Jörg Baschnagel. *Stochastic processes: From Physics to Finance*. Springer, 1999.

[17] Fischer Black and Myron Scholes. "The pricing of options and corporate liabilities". In: *Journal of political economy* 81.3 (1973), pp. 637–654.

[18] RC Merton. "Theory of rational option pricing". In: *Bell J. Econ. Management Science* 4 (1973).

[19] Tamirat Temesgen Dufera. "Fractional Brownian motion in option pricing and dynamic delta hedging: Experimental simulations". In: *The North American Journal of Economics and Finance* 69 (2024), p. 102017.

[20] Rama Cont. "Empirical properties of asset returns: stylized facts and statistical issues". In: *Quantitative finance* 1.2 (2001), p. 223.

[21] Rosario N Mantegna and H Eugene Stanley. *Introduction to econophysics: correlations and complexity in finance*. Cambridge university press, 1999.

[22] Paul A Samuelson. "Rational theory of warrant pricing". In: *Henry P. McKean Jr. Selecta*. Springer, 1965, pp. 195–232.

[23] Tiziana Di Matteoa, Tomaso Aste, and Michele M Dacorogna. "Using the scaling analysis to characterize financial markets". In: *arXiv preprint cond-mat/0302434* (2004).

[24] Tiziana Di Matteo, Tomaso Aste, and Michel M Dacorogna. "Long-term memories of developed and emerging markets: Using the scaling analysis to characterize their stage of development". In: *Journal of banking & finance* 29.4 (2005), pp. 827–851.

[25] Christian Bender, Tommi Sottinen, and Esko Valkeila. "Arbitrage with fractional Brownian motion?" In: *Theory of stochastic processes* 13.1 (2007), pp. 23–34.

[26] Ciprian Necula. "Option pricing in a fractional Brownian motion environment". In: *Available at SSRN 1286833* (2002).

[27] Jean-Philippe Bouchaud and Marc Potters. *Theory of financial risk and derivative pricing: from statistical physics to risk management*. Cambridge university press, 2003.

[28] Tyrone E Duncan, Yaozhong Hu, and Bozenna Pasik-Duncan. "Stochastic calculus for fractional Brownian motion I. Theory". In: *SIAM Journal on Control and Optimization* 38.2 (2000), pp. 582–612.

[29] Giovani L Vasconcelos. "A guided walk down wall street: an introduction to econophysics". In: *Brazilian Journal of Physics* 34.3b (2004), pp. 1039–1065.